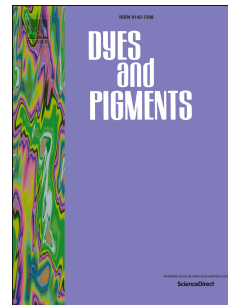


Accepted Manuscript

A structural study of Troger's base scaffold-based dyes for DSSC applications

Simona Urnikaite, Titas Braukyla, Artiom Magomedov, Egidijus Kamarauskas, Tadas Malinauskas, Vytautas Getautis



PII: S0143-7208(16)31509-1

DOI: [10.1016/j.dyepig.2017.04.012](https://doi.org/10.1016/j.dyepig.2017.04.012)

Reference: DYPI 5908

To appear in: *Dyes and Pigments*

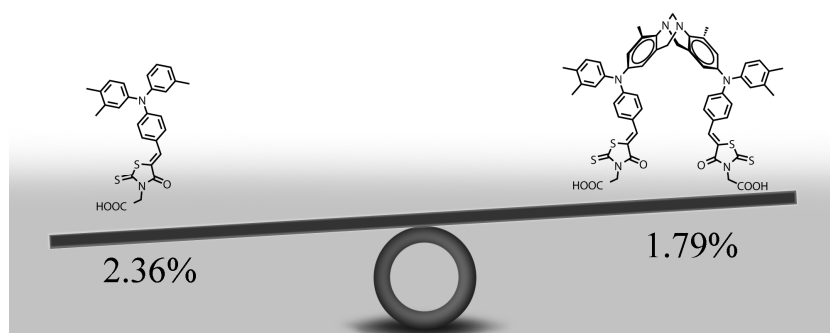
Received Date: 31 December 2016

Revised Date: 8 April 2017

Accepted Date: 10 April 2017

Please cite this article as: Urnikaite S, Braukyla T, Magomedov A, Kamarauskas E, Malinauskas T, Getautis V, A structural study of Troger's base scaffold-based dyes for DSSC applications, *Dyes and Pigments* (2017), doi: 10.1016/j.dyepig.2017.04.012.

This is a PDF file of an unedited manuscript that has been accepted for publication. As a service to our customers we are providing this early version of the manuscript. The manuscript will undergo copyediting, typesetting, and review of the resulting proof before it is published in its final form. Please note that during the production process errors may be discovered which could affect the content, and all legal disclaimers that apply to the journal pertain.



ACCEPTED MANUSCRIPT

A structural study of Troger's base scaffold-based dyes for DSSC applications

Simona Urnikaite^a, Titas Braukyla^a, Artiom Magomedov^a, Egidijus Kamarauskas^b, Tadas Malinauskas^a,
and Vytautas Getautis^{a*}

^a Department of Organic Chemistry, Kaunas University of Technology, Radvilenu pl. 19, LT-50254,
Kaunas, Lithuania

^b Department of Solid State Electronics, Vilnius University, Sauletekio 9, Vilnius, 10222, Lithuania.

Abstract

Three Troger's base scaffold-based metal-free sensitizers **TD1**, **TD2** and **TD3** with triphenylamine donor and rhodanine-3-acetic acid as an acceptor/anchoring group were designed and synthesized for dye-sensitized solar cells. The sensitizer series was designed to investigate the influence of the poly[n]enic (from n = 0 to 2) backbones and their anchoring effect in DSSCs. Optical, electrochemical and photovoltaic properties were compared with analogues dyes **D1-D3** possessing one anchoring group. It has been proven that the extended polymethine chains ensure flexibility of these units and inspire the interaction between two chromophores promoting aggregate formation in these Troger's base-based dyes.

Keywords

Dye-Sensitized Solar Cells; Polymethine Dyes; Troger's Base; Anchoring Group; Titanium Dioxide.

1. Introduction

Among the emerging photovoltaic technologies, dye-sensitized solar cells (DSSCs) have attracted significant attention as one of the promising energy harvesting devices since the report of Ru-based

24 photosensitizers [1]. After two decades of research and development, DSSCs with iodide/triiodide (I/I_3^-)
25 liquid electrolyte have achieved record power conversion efficiency (PCE) over 13% based on Zn-
26 porphyrin complex dyes [2,3]. Compared with them, metal-free organic dyes have such advantages as
27 relatively lower production cost, facile synthetic methodologies and high molar extinction coefficient [4].
28 An impressive cell efficiency of 12.5% achieved by a novel metal-free alkoxy-silyl carbazole dye
29 ADEKA-1 (Fig. 1) demonstrated that metal-free dyes could be promising sensitizers for realizing highly
30 efficient DSSCs [5]. Towards the realization of higher photovoltaic performance and durability in
31 DSSCs, the development of the sensitizing dyes is one of the most important approaches.

32 It is well known that most of the excellent sensitizers have the donor- π -acceptor (D- π -A) structures
33 which facilitate effective photoinduced intramolecular charge transfer across the molecule [6]. However,
34 the single 1D- π -1A sensitizer often has a rod-shaped structure, which may cause undesirable dye
35 aggregation and charge recombination [7]. To enhance the photovoltaic performance in DSSCs,
36 considerable efforts have been devoted to optimize the structure of the organic dyes, such as increasing
37 the amount of anchoring groups and/or extending π -conjugation to increase the molar extinction
38 coefficient of the absorption band, which can improve the light harvesting ability of the dyes [4a,8]. The
39 dye containing double/multiple anchor groups exhibited a unique advantage of stronger bonding with the
40 TiO_2 surface. Strong binding not only improves adsorption but also leads to red shift in absorption,
41 efficient charge injection [4a,9] and photocurrent generation [4a,10].

42 For an efficient dye, choosing an appropriate anchoring group moiety is particularly important. For
43 example, di-anchoring N719 dye gives higher cell efficiency than the protonated N3 dye with quadri-
44 anchoring groups (Fig. 1), which is attributed to the effect of the bound dye on the energy of the TiO_2
45 conducting band [11]. In recent years, the importance of anchoring groups for photovoltaic applications
46 was investigated by several research groups. Jia and Zheng reported that the PCE of the DSSC based on

47 Y-shaped D- π -(A)₂ type phenthiozine dye ZJA2 (4.55%) was 67% higher than the DSSC based on single
48 1D- π -1A sensitizer ZJA1 (2.72%, Fig. 1) [7]. Designed DSSCs of Abbotto et al. yielded power
49 conversion efficiency up to 5.7% (4.9% with ionic liquid electrolyte) with increased photocurrent and
50 enhanced stability under 1 sun conditions caused by the di-anchoring groups [12]. Sirohi and Lee
51 concluded that the di-anchoring moiety in dye KS-5 caused strong binding to TiO₂ which forced the dye
52 molecule to assume a non-planar conformation, thereby minimizing aggregation [13]. This factor together
53 with an extended conjugated framework led to about 1.5 times higher efficiency of KS-5 compared to
54 parent dye L1 (Fig. 1). Recently Cao et al., reported the novel metal-free organic dye bearing two
55 symmetric double donor-acceptor segments with an impressive power conversion efficiency, which is
56 22% higher than that of the mono-anchoring dye based counterpart [4a]. However, the same scientific
57 group obtained lower photovoltaic performance of di-anchoring phenothiazine based dye DP-2 compared
58 to its counterpart mono-anchoring dye SP (Fig. 1) [14]. This new dye featuring A-D- π -D-A configuration
59 with extended conjugation showed a higher molar extinction coefficient (ϵ), but exhibited π -stacked
60 aggregation on the TiO₂ surface, resulting in low efficiency of electron injection.

61

62

Insert Figure 1

63

64 In our previous work [15], we presented a novel A- π -D- π -A metal-free organic dye D7 (Fig. 1) with
65 two anchoring groups for solid state DSSC (ssDSSC) with spiro-OMeTAD as hole transporting material
66 (HTM). As one would expect, D7 demonstrated the highest extinction coefficient of all investigated D- π -
67 A hydrazone dyes in that study, mostly due to the presence of two electron accepting units and larger
68 change in the electronic charge distribution occurring during excitation. The device based on the
69 sensitizer D7 had the strongest and widest light absorbance from the whole series. However, the external

70 quantum efficiency and ssDSSC performance decreased more than 50% compared with analogues
71 sensitizers possessing one anchoring group. We concluded that the D-(π -A)₂ molecule has a rod-shaped
72 structure, which might cause undesirable dye aggregation promoted by carboxylic acid moieties not
73 attached to the TiO₂ surface. The unbound anchoring group could serve as a charge recombination in site
74 between the HTM and dye layers, reducing the performance on the ssDSSC cell.

75 In the current work, we synthesized three Troger's base (TB) scaffold-based metal-free sensitizers
76 **TD1**, **TD2** and **TD3** (Fig. 2) with a triphenylamine donor group and rhodanine-3-acetic acid unit as the
77 acceptor/anchoring group to investigate their di-anchoring effect in DSSCs. TB being a V-shaped C₂-
78 symmetric chiral molecule possesses many interesting features. TB analogues have found applications as
79 building blocks in the fields of supramolecular chemistry [16], molecular recognition [17], catalysis,
80 enzyme inhibitors [18], also as a central linking unit in the synthesis of HTMs [19]. The TB structure
81 allows it to be used as a core and provide angle ($\sim 90^\circ$) orientation for the conjugated π systems conjoined
82 to it [20]. The non-planar structure of the TB and presence of two carboxyl groups should ensure two
83 separate channels for charge transfer to TiO₂ and increase in overall device efficiency. Analogues dyes
84 **D1**, **D2** and **D3** (Fig. 1) with one anchoring group were synthesized for comparison.

85

86 *Insert Figure 2*

87

88 **2. Experimental details**

89 *2.1 General*

90 The solvents (tetrahydrofuran (THF), 1,4-dioxane, dimethyl sulfoxide (DMSO) and toluene) were dried
91 by standard procedures. Other reagents were purchased from Aldrich and TCI Europe and used without
92 further purification. 2-(4-Bromophenyl)-5,5-dimethyl-1,3-dioxane (**14**) [21] and 2,8-dibromo-4,10-

93 dimethyl-6*H*,12*H*-5,11-methanodibenzo[*b,f*][1,5]diazocine [22] were synthesized according to the earlier
94 reported procedures. Reactions which required the use of anhydrous, inert-atmosphere techniques were
95 carried out under inert atmosphere (argon). Reactions were monitored by using TLC on ALUGRAM SIL
96 G/UV254 plates and chromatographic separations were performed with silica gel (grade 9385, 230–400
97 mesh, 60 Å, Aldrich). ¹H (400 MHz) and ¹³C (100 MHz) NMR spectra were recorded at room
98 temperature with a Bruker Avance III 400 spectrometer. The chemical shifts, expressed in ppm, were
99 relative to tetramethylsilane (TMS). Infrared spectra were recorded on a Perkin Elmer Spectrum One
100 spectrometer using KBr pellets. UV-Vis spectra were recorded on Perkin Elmer Lambda 35 UV/Vis
101 spectrometer. Fluorescence (FL) of the investigated compounds in dilute DMSO solutions was measured
102 using an Edinburgh Instruments Fluorescence Spectrometer FLS920. Melting points were determined
103 using an electrothermal MEL-TEMP capillary melting point apparatus. Elemental analysis (C, H, and N)
104 was done using Exeter Analytical CE-440 elemental analyser, Model 440 C/H/N/.

105

106 *2.2 Cyclic-Voltammetry Measurements*

107 The electrochemical studies were carried out by a three-electrode assembly cell from Bio-Logic SAS
108 potentiostat-galvanostat. The measurements were carried out with a glassy carbon electrode in THF
109 solutions containing 0.1 M tetrabutylammonium hexafluorophosphate as electrolyte, Pt as the reference
110 and counter electrodes at a scan rate of 50 mV s⁻¹. Each measurement was calibrated with ferrocene (Fc).

111

112 *2.3 Ionization Potential Measurements*

113 The ionization potential *I*_p of the layers of the synthesized compounds was measured by the electron
114 photoemission in air method [23,24]. The samples for the ionization potential measurement were
115 prepared by dissolving materials in CHCl₃ and were coated on Al plates precoated with a ~0.5 μm thick

116 methylmethacrylate and methacrylic acid copolymer adhesive layer. The thickness of the transporting
117 material layer was 0.5–1 μm . Usually the photoemission experiments are carried out in vacuum and high
118 vacuum is one of the main requirements for these measurements. If the vacuum is not high enough, the
119 sample surface oxidation and gas adsorption influence the measurement results. In our case, however, the
120 organic materials investigated are stable enough to oxygen and the measurements may be carried out in
121 air. The samples were illuminated with monochromatic light from a quartz monochromator with
122 deuterium lamp. The power of the incident light beam was $(2-5)\cdot 10^{-8}$ W. A negative voltage of -300 V
123 was supplied to the sample substrate. The counter-electrode with a 4.5×15 mm^2 slit for illumination was
124 placed at 8 mm distance from the sample surface. The counter-electrode was connected to the input of the
125 BK2–16 type electrometer, working in the open input regime, for the photocurrent measurement. A 10^{-15}
126 $- 10^{-12}$ A strong photocurrent was flowing in the circuit under illumination. The photocurrent I is strongly
127 dependent on the incident light photon energy $h\nu$. The $I^{0.5}=f(h\nu)$ dependence was plotted. Usually the
128 dependence of the photocurrent on incident light quanta energy is well described by a linear relationship
129 between $I^{0.5}$ and $h\nu$ near the threshold. The linear part of this dependence was extrapolated to the $h\nu$ axis
130 and the I_p value was determined as the photon energy at the interception point.

131

132 *2.4 Computational Details*

133 The theoretical calculations were performed using TURBOMOLE version 7.0 software [25a]. The
134 molecular structure of the investigated compounds was optimized using Becke's three parameter
135 functional, B3LYP [25b,c] and the def2-SVP [25d,e] basis set in vacuum. Optimized structures and the
136 molecular orbitals were visualized with TmoleX version 4.1 software [25f].

137

138 *2.5 Solar cell assembly*

139 TiO₂ photo-electrodes were prepared on fluorine-doped tin oxide (FTO) glass, which initially was
140 cleaned in ultrasonic bath with detergent, water, acetone and ethanol for 30 min respectively. Then a
141 screen printing technique was used to prepare mesoporous TiO₂ films with an area of 5 × 5 mm². The
142 film consists of one transparent layer (8 μm) which was printed with colloidal TiO₂ paste (Dyename
143 GPS-30TS) and one 4 μm light-scattering layer (Dyename paste DN-GPS-22OS). Before printing the
144 second layer the film was dried at 125 °C for 6 min. Afterwards the electrodes were sintered in an oven
145 (Nabertherm Controller P320) in an air atmosphere using a temperature gradient program with four levels
146 at 180 °C (15 min), 320 °C (15 min), 390 °C (15 min) and 500 °C (30 min). Prior to the dye-sensitization
147 the electrodes were post treated with 40 mM TiCl₄ solution for 30 min, followed by heating at 500 °C for
148 30 min. At a temperature of 90 °C the electrodes were immersed in a dye bath for 18 h containing either
149 **D1** (0.5 mM), **D2** (0.5 mM), **D3** (0.5 mM) in DCM and **TD1** (0.5 mM), **TD2** (0.5 mM), **TD3** (0.5 mM) in
150 DCM:MeOH (4:1 v/v), or N719 (0.3 mM) and D35 (0.2 mM) in tert-butanol: acetonitrile (1:1 v/v). Any
151 non-attached dye was removed with solvent used for the dye bath. Counter electrodes were prepared by
152 depositing 10 μL of a H₂PtCl₆ solution in ethanol (5 mM) to FTO glass substrates followed by heating in
153 air at 400 °C for 30 min. Solar cells were assembled by sandwiching the photoelectrode and the counter
154 electrode using a 25 μm thick thermoplastic Surlyn frame. An electrolyte solution was then injected
155 through a hole predrilled in the counter electrode by vacuum back filling and the cell was sealed with
156 thermoplastic Surlyn cover and a microscope glass coverslip. The electrolyte consists of LiI (0.1 M), I₂
157 (0.05 M), 1-butyl-3-methylimidazolium iodide (BMII, 0.6 M) and 4-tert butylpyridine (TBP, 0.5 M) in
158 acetonitrile. Three solar cells were made with every dye.

159

160 *2.6 Solar cells characterization*

161 Current-voltage (IV) characteristics were determined by using a combination of a source measurement
162 unit (Keithley 2400) and a solar simulator (Newport, model 91160). The solar simulator provided light
163 with AM 1.5 G spectral distribution and was calibrated to an intensity of 100 mW cm^{-2} using a certified
164 reference solar cell (Fraunhofer ISE). On top of the DSC a black metal mask with an aperture of 5×5
165 mm^2 was applied.

166 Incident photon-to-current conversion efficiency (IPCE) spectra were measured with a computer-
167 controlled setup comprising a xenon light source (Spectral Products ASB-XE-175), a monochromator
168 (Spectral Products CM110) and a Keithley multimeter (model 2700). The IPCE spectra were calibrated
169 using a certified reference solar cell (Fraunhofer ISE).

170

171 *2.7 Synthesis of dyes*

172 General procedure A: To a solution of the mixture of respective aldehyde (1 mmol) and tributyl(1,3-
173 dioxalan-2-ylmethyl)phosphonium bromide (1.1 mmol) in anhydrous tetrahydrofuran (3 mL) was added
174 sodium hydride (60% dispersed in mineral oil, 3.0 equiv.) under argon gas atmosphere, and the resulting
175 turbid solution was stirred at room temperature for 12 hours. The reaction was monitored by TLC (3:1:21
176 v/v ethyl acetate/toluene/*n*-hexane). After completion of the reaction, the excess NaH was quenched
177 using 10% aq. HCl solution under cooling and the reaction mixture was brought to acidic pH. The
178 reaction mixture was then stirred further more at room temperature for 1 hour. The mixture was poured
179 into distilled water (10 mL) and extracted with ethyl acetate. The organic layer was dried over anhydrous
180 Na_2SO_4 , filtered off, and the solvent evaporated. The crude product was purified by column
181 chromatography [26].

182

183 General procedure **B**: To a solution of respective aryl aldehyde (1 mmol) in benzene (2 mL) were added
184 2,2-dimethyl-1,3-propanediol (1.2 mmol) and *p*-toluenesulfonic acid monohydrate (0.11 mmol). The
185 resulting mixture was stirred at 80 °C for 3 hours. After cooling to room temperature, the reaction was
186 quenched by adding distilled water, and then was extracted with ethyl acetate. The organic layer was
187 dried over anhydrous Na₂SO₄, filtered, and the solvent evaporated. The crude product was purified by
188 column chromatography [21].

189
190 General procedure **C**: Mixture of dioxane (2 mL) and water (4%) was purged with argon for 20 minutes.
191 Palladium(II) acetate (0.5%) and 2-dicyclohexylphosphino-2',6'-dimethoxybiphenyl (SPhos) (1.5%) were
192 added and mixture was heated to 80 °C for 2 min. Respective aryl halide (1 mmol), 3,4-dimethylaniline
193 (1.2 mmol) and sodium *tert*-butoxide (1.4 mmol) were added and the solution was refluxed for the
194 indicated time (30 min – 2 h) under Ar atmosphere. After termination of the reaction (TLC control), the
195 mixture was filtered through celite, distilled water were added and extraction was done with ethyl acetate.
196 The organic layer was dried over anhydrous Na₂SO₄, filtered, and the solvent evaporated. The crude
197 product was purified by column chromatography.

198
199 General procedure **D**: A solution of 2,8-dibromo-4,10-dimethyl-6*H*,12*H*-5,11-methanodibenzo[*b,f*][1,5]-
200 diazocine (1 mmol), respective amine (2.5 mmol) and anhydrous toluene (10 mL) was purged with argon
201 for 30 minutes. Afterwards, palladium(II) acetate (2%), tri-*tert*-butylphosphonium tetrafluoroborate
202 (2.7% mmol) and sodium *tert*-butoxide (3 mmol) were added and the solution was heated to reflux under
203 Ar atmosphere. After termination of the reaction (TLC control), the mixture was filtered through celite,
204 distilled water was added and extraction was done with ethyl acetate. The organic layer was dried over

205 anhydrous Na₂SO₄, filtered, and the solvent evaporated. The crude product was purified by column
206 chromatography.

207

208 General procedure **E**: A solution of respective protected aldehyde (1 mmol) in THF (3 mL) and 10% aq.
209 HCl solution (to acidic pH) was stirred at 40 °C for 1 hour. The solution was poured into saturated
210 NaHCO₃ solution and extracted with ethyl acetate. The combined organic phases were washed with brine,
211 dried with Na₂SO₄, and concentrated in vacuo. The crude residue was purified by column
212 chromatography.

213 General procedure **F**: The mixture of respective aldehyde (1 mmol), rhodanine-3-acetic acid (1.2–2.4
214 mmol) and ammonium acetate (0.3 mmol) was refluxed in either anhydrous toluene (26 mL) or glacial
215 acetic acid (3 mL). At the end of the reaction (TLC control), the mixture was cooled to room temperature.
216 The obtained crystals which formed upon standing were filtered off and washed or the crude product was
217 purified by column chromatography.

218

219

220 *E*-3-(4-Bromophenyl)-2-propenal (**1**)

221 Following general procedure **A**, a mixture of 4-bromobenzaldehyde (2 g, 10.8 mmol), tributyl(1,3-
222 dioxalan-2-ylmethyl)phosphonium bromide (4.39 g, 11.89 mmol) and NaH in anhydrous THF (30 mL)
223 was stirred at room temperature for 12 h. Product was purified by column chromatography using 3:1:21
224 v/v ethyl acetate/toluene/*n*-hexane as an eluent. Aldehyde **1** was obtained as light yellow crystals. Yield:
225 2.1 g (92%).

226 ¹H NMR (400 MHz, CDCl₃, ppm) δ 9.71 (d, *J* = 7.6 Hz, 1H), 7.60–7.54 (m, 2H), 7.49–7.37 (m, 3H),
227 6.71 (dd, *J* = 16.0, 7.6 Hz, 1H).

228 ^{13}C NMR (101 MHz, CDCl_3 , ppm) δ 193.46, 151.19, 132.86, 132.39, 129.79, 128.98, 125.70.

229 Anal. calcd. for $\text{C}_9\text{H}_7\text{BrO}$: C, 51.22; H, 3.34. Found: C, 51.23; H, 3.22.

230

231 *(2E,4E)-5-(4-bromophenyl)penta-2,4-dienal (2)*

232 Prepared from the aldehyde **1** (0.31 g, 1.48 mmol) in anhydrous THF (3.5 mL) following general
233 procedure A (tributyl(1,3-dioxalan-2-ylmethyl)phosphonium bromide: 0.60 g, 1.63 mmol). Reaction
234 mixture was refluxed for 5 h. The crude product was purified by column chromatography using 3:1:21
235 v/v ethyl acetate/toluene/*n*-hexane as an eluent to collect aldehyde **2** as light yellow crystals. Yield: 0.26 g
236 (73 %). The obtained data of product are in good agreement with reported data [27].

237 ^1H NMR (400 MHz, CDCl_3 , ppm) δ 9.64 (d, $J = 7.9$ Hz, 1H), 7.53 (d, $J = 8.5$ Hz, 2H), 7.38 (d, $J = 8.5$
238 Hz, 2H), 7.32–7.20 (m, 1H), 7.07–6.91 (m, 2H), 6.30 (dd, $J = 15.2, 7.9$ Hz, 1H).

239 ^{13}C NMR (101 MHz, CDCl_3 , ppm) δ 193.57, 151.54, 140.91, 134.50, 132.17, 132.07, 128.91, 126.81,
240 123.79.

241 Anal. calcd. for $\text{C}_{11}\text{H}_9\text{BrO}$: C, 55.72; H, 3.83. Found: C, 55.69; H, 3.80.

242

243 *(E)-2-(4-bromostyryl)-5,5-dimethyl-1,3-dioxane (3)*

244 Following general procedure B, a mixture of aldehyde **1** (1.79 g, 8.49 mmol), 2-dimethyl-1,3-propanediol
245 (1.06 g, 10.19 mmol) and *p*-toluenesulfonic acid monohydrate (0.17 g, 0.93 mmol) in benzene (17 mL)
246 was stirred at 80 °C for 3.5 h. Product was purified by column chromatography using 3:1:21 v/v ethyl
247 acetate/toluene/*n*-hexane as an eluent to collect protected aldehyde **3** as whitish crystals. Yield: 2.0 g
248 (80%).

249 ^1H NMR (400 MHz, CDCl_3 , ppm) δ 7.43 (d, $J = 8.5$ Hz, 2H), 7.26 (d, $J = 8.5$ Hz, 2H), 6.72 (d, $J = 16.2$
250 Hz, 1H), 6.21 (dd, $J = 16.2, 4.7$ Hz, 1H), 5.02 (d, $J = 4.2$ Hz, 1H), 3.69 (d, $J = 11.2$ Hz, 2H), 3.55 (d, $J =$
251 10.8 Hz, 2H), 1.24 (s, 3H), 0.76 (s, 3H).

252 ^{13}C NMR (101 MHz, CDCl_3 , ppm) δ 135.08, 132.19, 131.70, 128.36, 126.39, 122.03, 100.57, 30.24,
253 23.01, 21.93.

254 Anal. calcd. for $\text{C}_{14}\text{H}_{17}\text{BrO}_2$: C, 56.58; H, 5.77. Found: C, 56.60; H, 5.74.

255

256 *2-((1E,3E)-4-(4-bromophenyl)buta-1,3-dien-1-yl)-5,5-dimethyl-1,3-dioxane (4)*

257 Following general procedure B, a mixture of aldehyde **2** (1.84 g, 7.76 mmol), 2-dimethyl-1,3-propanediol
258 (0.97 g, 9.31 mmol) and *p*-toluenesulfonic acid monohydrate (0.16 g, 0.85 mmol) in benzene (16 mL)
259 was stirred at 80 $^\circ\text{C}$ for 3 h. Product was purified by column chromatography using 3:1:21 v/v ethyl
260 acetate/toluene/*n*-hexane as an eluent to collect protected aldehyde **4** as light yellow crystals. Yield: 1.6 g
261 (64%).

262 ^1H NMR (400 MHz, CDCl_3 , ppm) δ 7.43 (d, $J = 8.4$ Hz, 2H), 7.25 (d, $J = 7.6$ Hz, 2H), 6.81–6.68 (m,
263 1H), 6.62–6.48 (m, 2H), 5.83 (dd, $J = 15.3, 4.6$ Hz, 1H), 4.96 (d, $J = 4.6$ Hz, 1H), 3.68 (d, $J = 11.1$ Hz,
264 2H), 3.53 (d, $J = 10.8$ Hz, 2H), 1.23 (s, 3H), 0.76 (s, 3H).

265 ^{13}C NMR (101 MHz, CDCl_3 , ppm) δ 135.91, 133.23, 133.15, 131.74, 129.86, 128.47, 128.02, 121.59,
266 100.37, 30.22, 22.99, 21.93.

267 Anal. calcd. for $\text{C}_{16}\text{H}_{19}\text{BrO}_2$: C, 59.45; H, 5.93. Found: C, 59.41; H, 5.89.

268

269 *N-(4-(5,5-dimethyl-1,3-dioxan-2-yl)phenyl)-3,4-dimethylaniline (5)*

270 Compound **5** was synthesized following general method C: a mixture of $\text{Pd}(\text{OAc})_2$ (0.02 g, 0.09 mmol),
271 SPhos (0.11g, 0.27 mmol), 2-(4-bromophenyl)-5,5-dimethyl-1,3-dioxane **14** (5 g, 18.44 mmol), 3,4-

272 dimethylaniline (2.68 g, 22.13 mmol) and NaOt-Bu (2.48 g, 25.81 mmol) in anhydrous dioxane (35 mL)
273 was refluxed for 30 min. The crude product was purified by column chromatography using 0.5:14.5:10
274 v/v ethyl acetate/toluene/*n*-hexane and further purified by crystallization from 2-propanol to produce
275 diphenylamine **5** as white crystals. Yield: 4.62 g (80%).

276 ¹H NMR (400 MHz, CDCl₃, ppm) δ 7.36 (d, *J* = 8.5 Hz, 2H), 7.03–6.95 (m, 3H), 6.87 (d, *J* = 2.2 Hz, 1H),
277 6.82 (dd, *J* = 8.0, 2.4 Hz, 1H), 5.60 (s, 1H), 5.32 (s, 1H), 3.75 (d, *J* = 11.2 Hz, 2H), 3.63 (d, *J* = 10.6 Hz,
278 2H), 2.20 (s, 6H), 1.29 (s, 3H), 0.78 (s, 3H).

279 ¹³C NMR (101 MHz, CDCl₃, ppm) δ 144.52, 140.53, 137.54, 130.47, 130.36, 129.76, 127.25, 120.33,
280 116.65, 116.33, 101.92, 30.22, 23.11, 21.94, 19.96, 19.02.

281 Anal. calcd. for C₂₀H₂₅NO₂: C, 77.14; H, 8.09; N, 4.50. Found: C, 77.03; H, 8.00; N, 4.52.

282

283 *(E)*-*N*-(4-(2-(5,5-dimethyl-1,3-dioxan-2-yl)vinyl)phenyl)-3,4-dimethylaniline (**6**)

284 Prepared from compound **3** (2.02 g, 6.81 mmol), 3,4-dimethylaniline (1.00 g, 8.17 mmol) in the mixture
285 of dioxane (15 mL) and water (4 %) applying the same procedure as for general procedure C (Pd(OAc)₂:
286 0.007 g, 0.03 mmol; SPhos: 0.04 g, 0.10 mmol; NaOt-Bu: 0.92 g, 9.53 mmol). The resulting mixture was
287 stirred at reflux for 30 min. Product was separated by column chromatography using 3:1:21 v/v ethyl
288 acetate/toluene/*n*-hexane as an eluent and further purified by crystallization from 2-propanol to produce
289 diphenylamine **6** as pale yellow crystals. Yield: 1.60 g (70%).

290 ¹H NMR (400 MHz, CDCl₃, ppm) δ 7.27 (d, *J* = 8.6 Hz, 2H), 7.04 (d, *J* = 8.0 Hz, 1H), 6.94–6.84 (m,
291 4H), 6.70 (d, *J* = 16.1 Hz, 1H), 6.08 (dd, *J* = 16.1, 5.1 Hz, 1H), 5.65 (s, 1H), 5.02 (d, *J* = 4.9 Hz, 1H),
292 3.69 (d, *J* = 11.2 Hz, 2H), 3.56 (d, *J* = 10.9 Hz, 2H), 2.22 (s, 3H), 2.21 (s, 3H), 1.25 (s, 3H), 0.76 (s, 3H).

293 ¹³C NMR (101 MHz, CDCl₃, ppm) δ 144.20, 139.90, 137.63, 133.37, 130.37, 130.21, 128.05, 127.90,
294 122.34, 120.95, 116.89, 116.06, 101.47, 30.23, 23.05, 21.99, 20.00, 19.08.

295 Anal. calcd. for C₂₂H₂₇NO₂: C, 78.30; H, 8.06; N, 4.15. Found: C, 78.28; H, 8.06; N, 4.05.

296

297 *N*-(4-((1*E*,3*E*)-4-(5,5-dimethyl-1,3-dioxan-2-yl)buta-1,3-dien-1-yl)phenyl)-3,4-dimethylaniline (**7**)

298 Following general procedure C, a mixture of Pd(OAc)₂ (0.005 g, 0.02 mmol), SPhos (0.03 g, 0.07 mmol),
299 protected aldehyde **4** (1.58 g, 4.90 mmol), 3,4-dimethylaniline (0.71 g, 5.89 mmol) and NaOt-Bu (0.66 g,
300 6.87 mmol) in dioxane (10 mL) and water (4%) was refluxed for 1 h under Ar atmosphere. Product was
301 purified by column chromatography using 3:1:21 v/v ethyl acetate/toluene/*n*-hexane as an eluent and
302 further purified by crystallization from 2-propanol to produce diphenylamine **7** as pale yellow crystals.
303 Yield: 1.23 g (69%).

304 ¹H NMR (400 MHz, CDCl₃, ppm) δ 7.28 (d, *J* = 8.6 Hz, 2H), 7.04 (d, *J* = 8.0 Hz, 1H), 6.93 (d, *J* = 8.6
305 Hz, 2H), 6.91–6.82 (m, 2H), 6.68–6.49 (m, 3H), 5.77 (dd, *J* = 15.2, 4.9 Hz, 1H), 5.67 (s, 1H), 4.95 (d, *J* =
306 5.1 Hz, 1H), 3.67 (d, *J* = 11.1 Hz, 2H), 3.53 (d, *J* = 10.9 Hz, 2H), 2.22 (s, 3H), 2.21 (s, 3H), 1.23 (s, 3H),
307 0.75 (s, 3H). ¹³C NMR (101 MHz, CDCl₃, ppm) δ 143.84, 139.87, 137.60, 134.42, 134.19, 130.34,
308 130.13, 128.84, 127.73, 127.35, 124.80, 120.71, 116.67, 116.30, 100.85, 30.17, 22.98, 21.93, 19.95,
309 19.03.

310 Anal. calcd. for C₂₄H₂₉NO₂: C, 79.30; H, 8.04; N, 3.85. Found: C, 79.20; H, 8.08; N, 3.86.

311

312 (5*S*)-*N*²,*N*⁸-bis(4-(5,5-dimethyl-1,3-dioxan-2-yl)phenyl)-*N*²,*N*⁸-bis(3,4-dimethylphenyl)-4,10-dimethyl-
313 6*H*,12*H*-5,11-methanodibenzo[*b,f*][1,5]diazocine-2,8-diamine (**8**)

314 Following general procedure D, a mixture of diphenylamine **5** (2.18 g, 7.00 mmol), 2,8-dibromo-4,10-
315 dimethyl-6*H*,12*H*-5,11-methanodibenzo[*b,f*][1,5]diazocine (1.14 g, 2.80 mmol), Pd(OAc)₂ (0.012 g, 0.05
316 mmol), [P(*t*-Bu)₃H]BF₄ (0.023 g, 0.07 mmol) and NaOt-Bu (0.81 g, 8.39 mmol) in anhydrous toluene (20

317 mL) was heated at reflux for 2.5 h under Ar atmosphere. The crude product was purified by column
318 chromatography using 3:1:21 v/v ethyl acetate/toluene/*n*-hexane as an eluent to collect compound **8** as a
319 yellow solid. Yield: 1.8 g (76%).

320 ¹H NMR (400 MHz, CDCl₃, ppm) δ 7.32 (d, *J* = 8.5 Hz, 4H), 6.98 (d, *J* = 8.5 Hz, 6H), 6.86–6.74 (m,
321 6H), 6.48–6.44 (m, 2H), 5.33 (s, 2H), 4.40 (d, *J* = 17.0 Hz, 2H), 4.27 (s, 2H), 3.82 (d, *J* = 17.0 Hz, 2H),
322 3.76 (d, *J* = 11.1 Hz, 4H), 3.63 (d, *J* = 10.9 Hz, 4H), 2.24 (s, 6H), 2.21 (s, 6H), 2.15 (s, 6H), 1.30 (s, 6H),
323 0.79 (s, 6H).

324 ¹³C NMR (101 MHz, CDCl₃, ppm) δ 148.98, 145.48, 143.42, 141.19, 137.49, 133.78, 131.61, 131.33,
325 130.34, 129.07, 128.83, 128.27, 126.94, 126.11, 124.74, 122.93, 122.43, 119.66, 101.93, 77.77, 67.70,
326 54.99, 30.25, 23.13, 21.94, 19.87, 19.18, 17.03.

327 Anal. calcd. for C₅₇H₆₄N₄O₄: C, 78.77; H, 7.42; N, 6.45. Found: C, 78.78; H, 7.39; N, 6.45.

328

329 *(5S)-N²,N⁸-bis(4-((E)-2-(5,5-dimethyl-1,3-dioxan-2-yl)vinyl)phenyl)-N²,N⁸-bis(3,4-dimethylphenyl)-4,10-*
330 *dimethyl-6H,12H-5,11-methanodibenzo[*b,f*][1,5]diazocine-2,8-diamine (9)*

331 Prepared from the diphenylamine **6** (1.57 g, 4.67 mmol), 2,8-dibromo-4,10-dimethyl-6*H*,12*H*-5,11-
332 methanodibenzo[*b,f*][1,5]diazocine (0.76 g, 1.87 mmol) in the mixture of toluene (34 mL), Pd(OAc)₂
333 (0.008 g, 0.04 mmol), [P(*t*-Bu)₃H]BF₄ (0.015 g, 0.05 mmol) and NaO*t*-Bu (0.54 g, 5.60 mmol) applying
334 the same procedure as for general procedure D. The resulting mixture was stirred at reflux for 1 h.
335 Product was purified by column chromatography using 3:1:21 v/v ethyl acetate/toluene/*n*-hexane as an
336 eluent to collect compound **9** as light yellow crystals. Yield: 1.37 g (80%).

337 ¹H NMR (400 MHz, CDCl₃, ppm) δ 7.28–7.12 (m, 9H), 7.02 (d, *J* = 8.1 Hz, 2H), 6.90–6.78 (m, 5H), 6.69
338 (d, *J* = 16.1 Hz, 2H), 6.49 (d, *J* = 2.3 Hz, 2H), 6.07 (dd, *J* = 16.1, 4.9 Hz, 2H), 5.01 (d, *J* = 4.7 Hz, 2H),

339 4.44 (d, $J = 17.0$ Hz, 2H), 4.28 (s, 2H), 3.85 (d, $J = 17.0$ Hz, 2H), 3.69 (d, $J = 11.1$ Hz, 4H), 3.55 (d, $J =$
340 10.9 Hz, 4H), 2.25 (s, 6H), 2.22 (s, 6H), 2.17 (s, 6H), 1.24 (s, 6H), 0.76 (s, 6H).

341 ^{13}C NMR (101 MHz, CDCl_3 , ppm) δ 148.32, 145.08, 143.01, 141.50, 137.63, 133.90, 133.06, 131.86,
342 130.41, 128.88, 128.81, 127.54, 126.60, 125.23, 123.11, 122.92, 121.62, 120.16, 101.24, 67.57, 54.87,
343 30.18, 22.99, 21.94, 19.88, 19.20, 17.03.

344 Anal. calcd. for $\text{C}_{61}\text{H}_{68}\text{N}_4\text{O}_4$: C, 79.53; H, 7.44; N, 6.08. Found: C, 79.53; H, 7.40; N, 6.05.

345 (*5S*)- N^2, N^8 -bis(4-((*1E,3E*)-4-(5,5-dimethyl-1,3-dioxan-2-yl)buta-1,3-dien-1-yl)phenyl)- N^2, N^8 -bis(3,4-
346 dimethylphenyl)-4,10-dimethyl-6*H*,12*H*-5,11-methanodibenzo[*b,f*][1,5]diazocine-2,8-diamine (**10**)

347 Following general procedure D, a mixture of diphenylamine **7** (1.20 g, 3.30 mmol), 2,8-dibromo-4,10-
348 dimethyl-6*H*,12*H*-5,11-methanodibenzo[*b,f*][1,5]diazocine (0.54 g, 1.32 mmol), $\text{Pd}(\text{OAc})_2$ (0.006 g, 0.03
349 mmol), $[\text{P}(t\text{-Bu})_3\text{H}]\text{BF}_4$ (0.011 g, 0.03 mmol) and NaOt-Bu (0.38 g, 3.96 mmol) in anhydrous toluene (30
350 mL) was heated at reflux for 3.5 h under Ar atmosphere. The crude product was purified by column
351 chromatography using 3:22 v/v acetone/*n*-hexane as an eluent to collect compound **10** as a yellow solid.
352 Yield: 1.4 g (45%).

353 ^1H NMR (400 MHz, CDCl_3): $\delta = 7.25$ (d, $J = 8.6$ Hz, 4H), 7.05 (d, $J = 8.1$ Hz, 2H), 6.96–6.30 (m, 11H),
354 6.71–6.49 (m, 7H), 5.79 (dd, $J = 15.0, 4.9$ Hz, 2H), 4.98 (d, $J = 4.9$ Hz, 2H), 4.52 (d, $J = 16.8$ Hz, 2H),
355 4.38 (s, 2H), 3.90 (d, $J = 17.0$ Hz, 2H), 3.70 (d, $J = 10.7$ Hz, 4H), 3.56 (d, $J = 11.0$ Hz, 4H), 2.30 (s, 6H),
356 2.26 (s, 6H), 2.20 (s, 6H), 1.26 (s, 6H), 0.78 (s, 6H).

357 ^{13}C NMR (101 MHz, CDCl_3): $\delta = 147.92, 144.96, 137.75, 134.23, 134.11, 133.98, 130.50, 127.81,$
358 127.35, 126.62, 125.70, 125.05, 122.95, 122.25, 100.82, 54.84, 30.22, 23.02, 21.97, 19.93, 19.25, 17.14.

359 Anal. calcd. for $\text{C}_{65}\text{H}_{72}\text{N}_4\text{O}_4$: C, 80.21; H, 7.46; N, 5.76. Found: C, 80.15; H, 7.43; N, 5.71.

360

361 4,4'-(((5*S*)-4,10-dimethyl-6*H*,12*H*-5,11-methanodibenzo[*b,f*][1,5]diazocine-2,8-diyl)bis((3,4-
362 dimethylphenyl)azanediyl))dibenzaldehyde (**11**)

363 Following general procedure E, product was purified by column chromatography using 1:4 v/v acetone/*n*-
364 hexane as an eluent to collect dialdehyde **11** as yellow crystals. Yield: 0.66 g (46%).

365 ¹H NMR (400 MHz, CDCl₃, ppm) δ 9.76 (s, 2H), 7.61 (d, *J* = 8.8 Hz, 4H), 7.11 (d, *J* = 8.0 Hz, 2H), 6.98–
366 6.78 (m, 10H), 6.61 (d, *J* = 2.1 Hz, 2H), 4.50 (d, *J* = 17.0 Hz, 2H), 4.29 (s, 2H), 3.90 (d, *J* = 17.1 Hz, 2H),
367 2.32 (s, 6H), 2.26 (s, 6H), 2.22 (s, 6H).

368 ¹³C NMR (101 MHz, CDCl₃, ppm) δ 190.32, 153.90, 143.49, 143.46, 141.46, 138.30, 134.71, 134.24,
369 131.32, 130.94, 129.39, 128.08, 128.02, 126.98, 124.40, 122.16, 117.78, 67.44, 54.78, 26.93, 19.91,
370 19.36, 17.11.

371 Anal. calcd. for C₄₇H₄₄N₄O₂: C, 81.00; H, 6.36; N, 8.04. Found: C, 81.02; H, 6.36; N, 8.00.

372
373 (2*E*,2'*E*)-3,3'-(((5*S*)-4,10-dimethyl-6*H*,12*H*-5,11-methanodibenzo[*b,f*][1,5]diazocine-2,8-diyl)bis((3,4-
374 dimethylphenyl)azanediyl))bis(4,1-phenylene))diacrylaldehyde (**12**)

375 Following general procedure E, product was purified by column chromatography using 1:4 v/v acetone/*n*-
376 hexane as an eluent to collect dialdehyde **12** as yellow crystals. Yield: 0.86 g (78%).

377 ¹H NMR (400 MHz, CDCl₃, ppm) δ 9.61 (d, *J* = 7.8 Hz, 2H), 7.40–7.32 (m, 6H), 7.09 (d, *J* = 8.1 Hz,
378 2H), 6.96–6.92 (m, 2H), 6.90–6.84 (m, 8H), 6.60–6.50 (m, 4H), 4.49 (d, *J* = 17.0 Hz, 2H), 4.29 (s, 2H),
379 3.89 (d, *J* = 17.1 Hz, 2H), 2.30 (s, 6H), 2.26 (s, 6H), 2.21 (s, 6H).

380 ¹³C NMR (101 MHz, CDCl₃, ppm) δ 193.78, 153.01, 151.36, 143.88, 142.83, 141.86, 138.11, 134.45,
381 133.59, 130.76, 129.82, 129.21, 127.57, 126.42, 125.34, 125.30, 123.94, 121.53, 119.31, 67.45, 54.77,
382 19.91, 19.32, 17.09.

383 Anal. calcd. for C₅₁H₄₈N₄O₂: C, 81.79; H, 6.46; N, 7.48. Found: C, 81.78; H, 6.45; N, 7.50.

384
385 (2*E*,2'*E*,4*E*,4'*E*)-5,5'-((((5*S*)-4,10-dimethyl-6*H*,12*H*-5,11-methanodibenzo[*b,f*][1,5]diazocine-2,8-
386 diyl)bis((3,4-dimethylphenyl)azanediyl))bis(4,1-phenylene))bis(penta-2,4-dienal) (**13**)
387 Following general procedure E, product was purified by column chromatography using 1:4 v/v THF/*n*-
388 hexane as an eluent to collect dialdehyde **13** as orange crystals. Yield: 0.8 g (70%).
389 ¹H NMR (400 MHz, CDCl₃, ppm) δ 9.57 (d, *J* = 8.0 Hz, 2H), 7.34–7.18 (m, 5H), 7.06 (d, *J* = 8.1 Hz,
390 2H), 6.95–6.79 (m, 15H), 6.55 (d, *J* = 2.1 Hz, 2H), 6.20 (dd, *J* = 15.1, 8.0 Hz, 2H), 4.47 (d, *J* = 17.0 Hz,
391 2H), 4.29 (s, 2H), 3.87 (d, *J* = 16.7 Hz, 2H), 2.28 (s, 6H), 2.25 (s, 6H), 2.20 (s, 6H).
392 ¹³C NMR (101 MHz, CDCl₃, ppm) δ 193.57, 153.00, 149.94, 144.38, 142.56, 142.38, 137.94, 134.27,
393 132.96, 130.66, 130.04, 129.11, 128.61, 127.62, 127.21, 125.94, 123.57, 123.37, 120.96, 120.47, 114.15,
394 67.55, 54.88, 19.90, 19.28, 17.08.
395 Anal. calcd. for C₅₅H₅₂N₄O₂: C, 82.47; H, 6.54; N, 6.99. Found: C, 82.45; H, 6.56; N, 7.01.
396 *Dye TD1*
397 Following general procedure F, a mixture of dialdehyde **11** (0.73 g, 1.05 mmol), rhodanine-3-acetic acid
398 (0.48 g, 2.52 mmol) and AcONH₄ (0.05 g, 0.63 mmol) was refluxed in anhydrous toluene (3 mL) for 12
399 h. The crude product was purified by column chromatography using 7:18 v/v acetone/*n*-hexane, 2:3 v/v
400 acetone/*n*-hexane and finally 3:22 v/v methanol/toluene to collect dye **TD1** as a red solid. Yield: 0.37 g
401 (34%), m.p. > 400°C. UV–vis (DMSO): λ_{max} (nm) 307 (ε = 36 382 M⁻¹ cm⁻¹), 475 (ε = 71 369 M⁻¹ cm⁻¹).
402 ¹H NMR (400 MHz, DMSO-*d*₆, ppm) δ 7.63 (s, 2H), 7.42 (d, *J* = 8.9 Hz, 4H), 7.15 (d, *J* = 8.2 Hz, 2H),
403 7.00–6.83 (m, 6H), 6.75 (d, *J* = 8.9 Hz, 4H), 6.70–6.62 (m, 2H), 4.48–4.37 (m, 6H), 4.21 (s, 2H), 3.97 (d,
404 *J* = 17.6 Hz, 2H), 2.28 (s, 6H), 2.21 (s, 6H), 2.17 (s, 6H).

405 ^{13}C NMR (101 MHz, DMSO- d_6 , ppm) 207.04, 193.22, 167.40, 167.33, 150.97, 143.68, 143.50, 141.12,
406 138.54, 134.81, 134.42, 133.40, 133.08, 131.45, 130.09, 128.14, 126.79, 124.77, 124.10, 122.39, 118.51,
407 117.73, 67.49, 54.50, 47.63, 31.16, 19.92, 19.38, 17.26.

408 IR (KBr, cm^{-1}): $\nu = 3394$ (OH); 3016 (aromatic CH); 2950, 2916, 2883 (aliphatic CH); 1698 ($2\times\text{C}=\text{O}$);
409 1575 (C=C); 1505 (C-C); 1324 (C=S); 1200, 1181 (C-N).

410 Anal. calcd. for $\text{C}_{57}\text{H}_{50}\text{N}_6\text{O}_6\text{S}_4$: C, 65.62; H, 4.83; N, 8.06. Found: C, 65.60; H, 4.85; N, 8.06.

411

412 Dye **TD2**

413 Following general procedure F, a mixture of dialdehyde **12** (0.29 g, 0.38 mmol), rhodanine-3-acetic acid
414 (0.18 g, 0.93 mmol) and AcONH_4 (0.01 g, 0.11 mmol) was refluxed in anhydrous toluene (8 mL) for 12
415 h. At the end of the reaction, the mixture was cooled to room temperature. Dark red crystals, formed
416 upon standing, were filtered off and washed with water (50 mL), toluene (50 mL) and finally with diethyl
417 ether (25 mL) to give dye **TD2**. Yield: 0.41 g (96%), m.p. 232-234 °C. UV-vis (DMSO): λ_{max} (nm) 298
418 ($\epsilon = 56\,510\text{ M}^{-1}\text{ cm}^{-1}$), 510 ($\epsilon = 44\,680\text{ M}^{-1}\text{ cm}^{-1}$).

419 ^1H NMR (400 MHz, DMSO- d_6 , ppm) δ 7.62–7.39 (m, 3H), 7.36–6.97 (m, 10H), 6.95–6.55 (m, 11H),
420 4.65 (s, 2H), 4.54 (s, 4H), 4.40 (s, 4H), 2.25 (s, 6H), 2.20 (s, 6H), 2.16 (s, 6H).

421 ^{13}C NMR (101 MHz, DMSO- d_6 , ppm) δ 203.31, 192.94, 174.26, 167.86, 167.80, 166.11, 152.26, 151.52,
422 150.49, 146.89, 144.09, 143.13, 143.02, 138.31, 137.82, 135.66, 131.32, 129.92, 129.37, 128.68, 127.65,
423 125.79, 119.60, 45.49, 36.41, 21.52, 19.92, 19.35, 17.26.

424 IR (KBr, cm^{-1}): $\nu = 3430$ (OH); 3033 (aromatic CH); 2966, 2922, 2850 (aliphatic CH); 1735 ($2\times\text{C}=\text{O}$);
425 1600, 1563 (C=C); 1505 (C-C); 1327 (C=S); 1192, 1162 (C-N).

426 Anal. calcd. for $\text{C}_{61}\text{H}_{54}\text{N}_6\text{O}_6\text{S}_4$: C, 66.89; H, 4.97; N, 7.67. Found: C, 66.89; H, 4.95; N, 7.67.

427

428 *Dye TD3*

429 Following general procedure F, a mixture of dialdehyde **13** (0.25 g, 0.31 mmol), rhodanine-3-acetic acid
430 (0.14 g, 0.74 mmol) and AcONH₄ (0.01 g, 0.10 mmol) was refluxed in anhydrous toluene (8 mL) for 12
431 h. At the end of the reaction, the mixture was cooled to room temperature. Dark violet crystals, formed
432 upon standing, were filtered off and washed with water (50 mL), methanol (50 mL) and finally with
433 diethyl ether (25 mL) to give target dye **TD3**. Yield: 0.27 g (76%), m.p. > 400°C. UV-vis (DMSO): λ_{max}
434 (nm) 302 ($\epsilon = 43\,360\text{ M}^{-1}\text{ cm}^{-1}$), 389 ($\epsilon = 23\,040\text{ M}^{-1}\text{ cm}^{-1}$), 526 ($\epsilon = 68\,550\text{ M}^{-1}\text{ cm}^{-1}$).

435 ¹H NMR (400 MHz, DMSO-*d*₆, ppm) δ 7.51 (d, $J = 11.9$ Hz, 2H), 7.35 (d, $J = 8.5$ Hz, 4H), 7.28–7.12 (m,
436 8H), 7.09 (d, $J = 8.2$ Hz, 2H), 6.93–6.64 (m, 8H), 6.56 (s, 2H), 6.51–6.39 (m, 2H), 4.61 (s, 4H), 4.38 (d, J
437 = 17.0 Hz, 2H), 4.18 (s, 2H), 3.90 (d, $J = 17.4$ Hz, 2H), 2.23 (s, 6H), 2.18 (s, 6H), 2.13 (s, 6H).

438 ¹³C NMR (101 MHz, DMSO-*d*₆, ppm) δ 192.51, 174.28, 167.77, 166.05, 149.46, 147.93, 144.46, 142.66,
439 142.07, 140.42, 138.14, 137.75, 134.68, 134.43, 133.17, 131.23, 129.81, 129.37, 129.08, 128.67, 127.37,
440 126.19, 125.81, 121.45, 120.33, 54.53, 45.89, 21.52, 19.92, 19.31, 17.25.

441 IR (KBr, cm⁻¹): $\nu = 3433$ (OH); 3033 (aromatic CH); 2946, 2916 (aliphatic CH); 1698 (2×C=O); 1600,
442 1545 (C=C); 1502 (C-C); 1309 (C=S); 1197, 1154 (C-N).

443 Anal. calcd. for C₆₅H₅₈N₆O₆S₄: C, 68.04; H, 5.10; N, 7.32. Found: C, 68.00; H, 5.12; N, 7.34.

444

445 *4-((3,4-dimethylphenyl)(*m*-tolyl)amino)benzaldehyde (15)*

446 Aldehyde **15** was synthesized following general method C: a mixture of Pd(OAc)₂ (0.009 g, 0.03 mmol),
447 SPhos (0.04g, 0.09 mmol), diphenylamine **5** (2 g, 6.42 mmol), 3-iodotoluene (1 mL, 7.71 mmol) and
448 NaOt-Bu (0.86 g, 8.99 mmol) in anhydrous dioxane (12 mL) was refluxed for 2 h. The crude product
449 was purified by column chromatography using 0.5:24.5 v/v THF/*n*-hexane as an eluent to collect
450 intermediate as light brown oil. Subsequently, it was applied for general procedure E. A light yellow

451 precipitate formed and was separated by extraction and concentration of the organic layer. Yield: 1.04 g
452 (55%).

453 ^1H NMR (400 MHz, CDCl_3 , ppm) δ 9.77 (s, 1H), 7.64 (d, $J = 8.8$ Hz, 2H), 7.26–7.18 (m, 1H), 7.10 (d, J
454 = 8.1 Hz, 1H), 7.01–6.85 (m, 7H), 2.30 (s, 3H), 2.26 (s, 3H), 2.21 (s, 3H).

455 ^{13}C NMR (101 MHz, CDCl_3 , ppm) δ 190.41, 153.77, 146.08, 143.70, 139.65, 138.21, 133.99, 131.31,
456 130.86, 129.46, 128.43, 127.86, 126.87, 125.91, 124.20, 123.40, 118.52, 21.40, 19.89, 19.33.

457 Anal. calcd. for $\text{C}_{22}\text{H}_{21}\text{NO}$: C, 83.78; H, 6.71; N, 4.44. Found: C, 83.73; H, 6.76; N, 4.45.

458

459 *(E)*-3-(4-((3,4-dimethylphenyl)(*m*-tolyl)amino)phenyl)acrylaldehyde (**16**)

460 Aldehyde **16** was prepared from the arylaldehyde **15** (0.60 g, 1.91 mmol), in anhydrous THF (7 mL)
461 applying general procedure A (tributyl(1,3-dioxolan-2-ylmethyl)phosphonium bromide: 0.78 g, 2.10
462 mmol). Reaction mixture was stirred for 3 h. The crude product was purified by column chromatography
463 using 3:1:21 v/v ethyl acetate/toluene/*n*-hexane as an eluent to collect compound **16** as a yellow solid.
464 Yield: 0.51 g (78%).

465 ^1H NMR (400 MHz, CDCl_3 , ppm) δ 9.64 (d, $J = 7.8$ Hz, 1H), 7.43–7.36 (m, 3H), 7.31–7.25 (m, 1H),
466 7.25–7.16 (m, 2H), 7.12 (d, $J = 8.0$ Hz, 1H), 7.02–6.88 (m, 5H), 6.60 (dd, $J = 15.8, 7.8$ Hz, 1H), 2.32 (s,
467 3H), 2.28 (s, 3H), 2.23 (s, 3H).

468 ^{13}C NMR (101 MHz, CDCl_3 , ppm) δ 193.82, 153.03, 151.24, 146.51, 144.12, 139.48, 138.07, 133.39,
469 130.74, 129.85, 129.32, 127.45, 126.25, 125.80, 125.53, 125.22, 123.79, 122.79, 120.13, 21.44, 19.93,
470 19.33.

471 Anal. calcd. for $\text{C}_{24}\text{H}_{23}\text{NO}$: C, 84.42; H, 6.79; N, 4.10. Found: C, 84.38; H, 6.76; N, 4.10.

472 *(2E,4E)*-5-(4-((3,4-dimethylphenyl)(*m*-tolyl)amino)phenyl)penta-2,4-dienal (**17**)

473 Compound **17** was prepared from the intermediate **16** (0.62 g, 1.81 mmol), in anhydrous THF (6 mL)
474 applying general method A (tributyl(1,3-dioxalan-2-ylmethyl)phosphonium bromide: 0.74 g, 1.99 mmol).
475 Reaction mixture was stirred for 1 h. The crude product was purified by column chromatography using
476 3:1:21 v/v ethyl acetate/toluene/*n*-hexane as an eluent to collect aldehyde **17** as a yellow solid. Yield:
477 0.56 g (84%).

478 ¹H NMR (400 MHz, CDCl₃, ppm) δ 9.57 (d, *J* = 8.0 Hz, 1H), 7.32 (d, *J* = 8.6 Hz, 2H), 7.28–7.12 (m,
479 4H), 7.06 (d, *J* = 8.0 Hz, 1H), 6.98–6.80 (m, 7H), 6.20 (dd, *J* = 15.1, 8.0 Hz, 1H), 2.27 (s, 3H), 2.24 (s,
480 3H), 2.19 (s, 3H).

481 ¹³C NMR (101 MHz, CDCl₃, ppm) δ 193.70, 153.15, 149.80, 146.93, 144.53, 142.62, 139.32, 137.92,
482 132.84, 130.64, 130.10, 129.21, 128.64, 127.98, 127.12, 125.76, 124.65, 123.53, 123.44, 122.32, 121.13,
483 21.45, 19.93, 19.30.

484 Anal. calcd. for C₂₆H₂₅NO: C, 84.98; H, 6.86; N, 3.81. Found: C, 84.94; H, 6.88; N, 3.84.

485

486 *Dye D1*

487 Following general procedure F, a mixture of aldehyde **15** (0.47 g, 1.50 mmol), rhodanine-3-acetic acid
488 (0.34 g, 1.80 mmol) and AcONH₄ (0.03 g, 0.45 mmol) was refluxed in anhydrous toluene (2 mL) for 12
489 h. The crude product was purified by column chromatography using 7:18 v/v acetone/*n*-hexane, 2:3 v/v
490 acetone/*n*-hexane and finally 3:22 v/v methanol/toluene to collect dye **D1** as a red solid. Yield: 0.31 g
491 (43%), m.p. 193-195 °C. UV-vis (DMSO): λ_{max} (nm) 307 (ε = 14 679 M⁻¹ cm⁻¹), 469 (ε = 37 956 M⁻¹ cm⁻¹).
492 ¹).

493 ¹H NMR (400 MHz, DMSO-*d*₆, ppm) δ 7.65 (s, 1H), 7.47 (d, *J* = 9.0 Hz, 2H), 7.32–7.22 (m, 1H), 7.18
494 (d, *J* = 8.1 Hz, 1H), 7.06–6.88 (m, 5H), 6.85 (d, *J* = 8.9 Hz, 2H), 4.47 (s, 2H), 2.26 (s, 3H), 2.22 (s, 3H),
495 2.18 (s, 3H). ¹³C NMR (101 MHz, DMSO-*d*₆, ppm) δ 193.31, 167.36, 150.71, 146.04, 143.64, 139.83,

496 138.54, 134.31, 133.31, 133.06, 131.40, 130.15, 128.01, 126.81, 126.35, 124.58, 124.54, 123.53, 119.19,
497 118.10, 67.49, 47.74, 21.40, 19.91, 19.37.

498 IR (KBr, cm^{-1}): $\nu = 3423$ (OH); 3033 (aromatic CH); 2919, 2850 (aliphatic CH); 1711 ($2\times\text{C}=\text{O}$); 1574
499 ($\text{C}=\text{C}$); 1506 (C-C); 1320, 1308 (C=S); 1200, 1180 (C-N).

500 Anal. calcd. for $\text{C}_{27}\text{H}_{24}\text{N}_2\text{O}_3\text{S}_2$: C, 66.37; H, 4.95; N, 5.73. Found: C, 66.35; H, 4.94; N, 5.74.

501

502 *Dye D2*

503 Following general procedure F, a mixture of aldehyde **16** (0.22 g, 0.66 mmol), rhodanine-3-acetic acid
504 (0.15 g, 0.79 mmol) and AcONH_4 (0.02 g, 0.19 mmol) was refluxed in glacial acetic acid (2 mL) for 2.5
505 h. The crude product was purified by column chromatography using 2:23 v/v methanol/toluene as an
506 eluent to collect dye **D2** as a red solid. Yield: 0.27 g (71%), m.p. 239-240 °C. UV-vis (DMSO): λ_{max} (nm)
507 304 ($\epsilon = 13\,270\ \text{M}^{-1}\ \text{cm}^{-1}$), 493 ($\epsilon = 37\,190\ \text{M}^{-1}\ \text{cm}^{-1}$).

508 ^1H NMR (400 MHz, $\text{DMSO-}d_6$, ppm) δ 7.57–7.42 (m, 3H), 7.31–7.08 (m, 3H), 6.97–6.76 (m, 8H), 4.39
509 (s, 2H), 2.23 (s, 3H), 2.20 (s, 3H), 2.16 (s, 3H).

510 ^{13}C NMR (101 MHz, $\text{DMSO-}d_6$, ppm) δ 192.94, 166.60, 149.96, 146.72, 145.61, 144.29, 138.27, 134.08,
511 133.42, 131.23, 130.02, 129.94, 129.37, 128.67, 128.35, 127.41, 125.96, 125.78, 123.90, 122.70, 122.26,
512 121.29, 120.43, 48.22, 21.42, 19.91, 19.32.

513 IR (KBr): $\nu = 3412$ (OH); 3033 (aromatic CH); 2918, 2850 (aliphatic CH); 1704 ($2\times\text{C}=\text{O}$); 1600, 1565
514 ($\text{C}=\text{C}$); 1498 (C-C); 1316, 1300 (C=S); 1197, 1160 (C-N).

515 Anal. calcd. for $\text{C}_{29}\text{H}_{26}\text{N}_2\text{O}_3\text{S}_2$: C, 67.68; H, 5.09; N, 5.44. Found: C, 67.65; H, 5.10; N, 5.47.

516

517 *Dye D3*

518 Following general procedure F, a mixture of aldehyde **17** (0.25 g, 0.69 mmol), rhodanine-3-acetic acid
519 (0.16 g, 0.83 mmol) and AcONH₄ (0.02 g, 0.20 mmol) was refluxed in glacial acetic acid (2.5 mL) for 45
520 min. The crude product was purified by column chromatography using 2:23 v/v methanol/toluene as an
521 eluent to collect dye **D3** as a red solid. Yield: 0.20 g (54%), m.p. 199-200 °C. UV-vis (DMSO): λ_{max} (nm)
522 308 ($\epsilon = 14\,740\text{ M}^{-1}\text{ cm}^{-1}$), 503 ($\epsilon = 26\,190\text{ M}^{-1}\text{ cm}^{-1}$).

523 ¹H NMR (700 MHz, DMSO-*d*₆, ppm) δ 7.48–7.39 (m, 3H), 7.23–7.10 (m, 4H), 7.08–7.00 (m, 1H), 6.94–
524 6.78 (m, 7H), 6.50–6.43 (m, 1H), 4.38 (s, 2H), 2.23 (s, 3H), 2.20 (s, 3H), 2.16 (s, 3H).

525 ¹³C NMR (176 MHz, DMSO-*d*₆, ppm) δ 192.55, 166.50, 149.05, 147.03, 146.92, 144.58, 139.69, 139.44,
526 138.19, 131.20, 129.89, 129.37, 128.98, 128.68, 127.26, 126.59, 125.79, 125.59, 125.38, 125.01, 123.74,
527 122.74, 122.33, 121.14, 48.20, 21.52, 21.45, 19.93, 19.30.

528 IR (KBr): $\nu = 3423$ (OH); 3033 (aromatic CH); 2916, 2866 (aliphatic CH); 1703 (2×C=O); 1600, 1566,
529 1545 (C=C); 1503 (C-C); 1314 (C=S); 1197, 1154 (C-N).

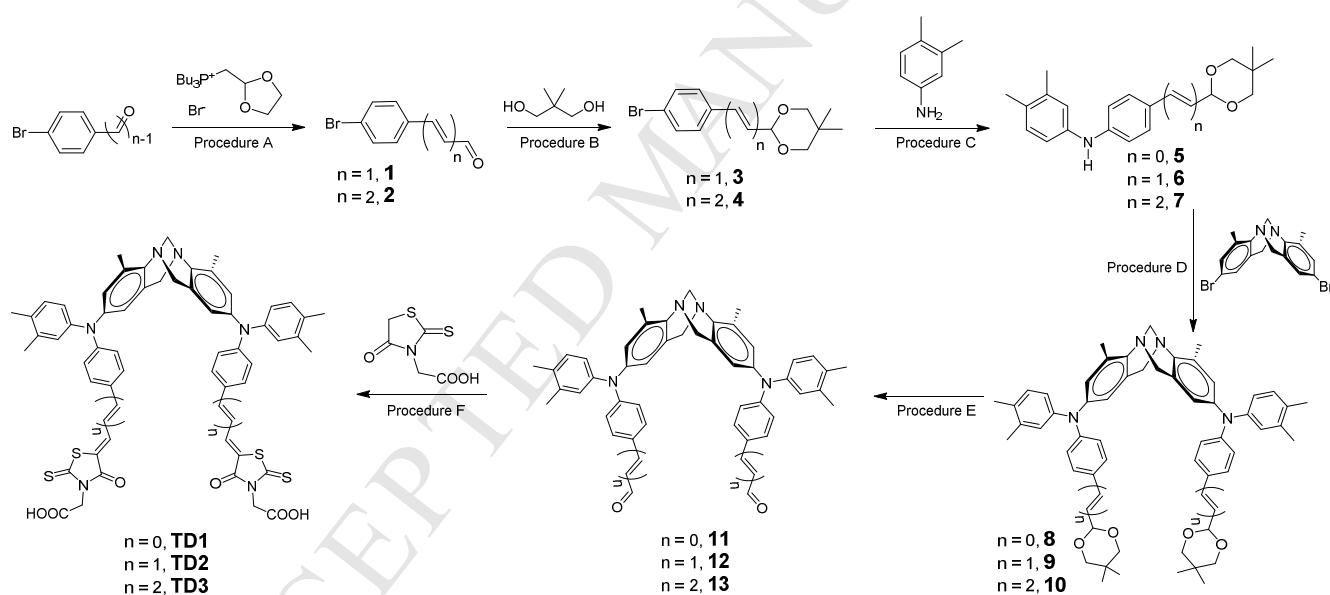
530 Anal. calcd. for C₃₁H₂₈N₂O₃S₂: C, 68.86; H, 5.22; N, 5.18. Found: C, 68.85; H, 5.23; N, 5.15.

531 3. Results and discussion

532 3.1 Synthesis

533 The new metal-free di-anchoring organic dyes based on TB scaffold **TD1**, **TD2** and **TD3** were
534 synthesized according to a six-step reaction as described in Scheme 1. Initially, Horner-Wittig
535 condensation was made to increase the polyenic chain (from n = 0 to 2). The yield of 70–80% were
536 achieved by palladium-catalyzed cross-coupling reaction between protected aldehydes **3**, **4** and 3,4-
537 dimethylaniline. The obtained corresponding diphenylamines **5**, **6** and **7** were then reacted with 2,8-
538 dibromo-4,10-dimethyl-6*H*,12*H*-5,11-methanodibenzo[*b,f*][1,5]diazocine [22] in the presence of
539 palladium(II) acetate, tri-*tert*-butylphosphonium tetrafluoroborate and sodium *tert*-butoxide to provide
540 intermediates based on TB scaffold **8**, **9** and **10**. After deprotection, the obtained penultimate dialdehydes

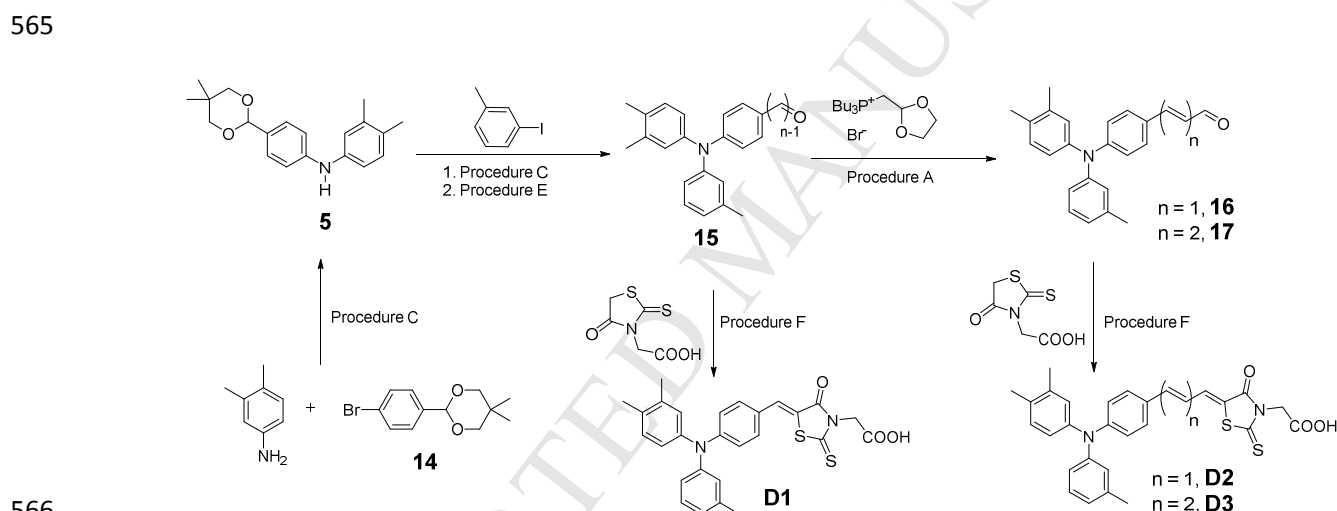
541 **11–13** were a common synthon, which were condensed with rhodanine-3-acetic acid to give sensitizers
 542 **TD1**, **TD2** and **TD3**. These new dyes were prepared in moderate to high yields and their chemical
 543 structures were confirmed by ^1H and ^{13}C NMR spectroscopy. Pattern of the signals in the interval of
 544 3.75–4.50 ppm in the ^1H NMR spectrum is essential for the methylene bridge identification, proving the
 545 presence of the TB core. Each ^1H NMR spectrum of **TD1–TD3** shows two doublets near each margin of
 546 the mentioned interval and these two doublets signify that the protons in bridging methylene part (Ar-
 547 $\text{CH}_2\text{-N}$) are magnetically nonequivalent due to the rigid structure of the TB. As a contrasting example to
 548 this, signals of two protons of the other bridging methylene carbon ($\text{N-CH}_2\text{-N}$) can be observed as a
 549 singlet at *ca.* 4.20 ppm in these spectrums.



552 **Scheme 1.** Synthesis of di-anchoring dyes based on TB scaffold **TD1**, **TD2** and **TD3**. Reagents and
 553 conditions: (A) i) THF, NaH 60%, r.t.; ii) 10% aq. HCl, r.t. (B) Benzene, cat., 80 °C. (C) Pd(OAc)₂,
 554 SPhos, H₂O, NaO*t*-Bu, dioxane, reflux. (D) Pd(OAc)₂, [P(*t*-Bu)₃H]BF₄, NaO*t*-Bu, toluene, reflux. (E)
 555 10% aq. HCl, 40 °C. (F) AcONH₄, toluene, reflux.

556

557 Dyes **D1**, **D2** and **D3** (Fig. 2) possessing one anchoring group were synthesized for comparison.
 558 Firstly, compound **14** was prepared according to reported procedure [21]. Then, the diphenylamine
 559 bearing the protected aldehyde group has been synthesized and equipped with 3-iodotoluene using the
 560 palladium-catalyzed Buchwald-Hartwig C–N cross-coupling reactions, to form the intermediate aldehyde
 561 **15**. The Knoevenagel condensation of the obtained aldehyde with rhodanine-3-acetic acid in glacial acetic
 562 acid gave dye **D1**. In parallel, Horner-Wittig condensation of aldehyde **15** with 1.1 equivalents of
 563 tributyl(1,3-dioxolan-2-ylmethyl)phosphonium bromide gave aldehyde **16** in 78% yield. Another
 564 vinylogation and subsequent Knoevenagel condensation produced dyes **D2** and **D3** (Scheme 2).



Scheme 2. Synthesis of mono-anchoring dyes **D1**, **D2** and **D3**. Reagents and conditions: (A) i) THF,

NaH 60%, r.t.; ii) 10% aq. HCl, r.t. (C) Pd(OAc)₂, SPhos, H₂O, NaOt-Bu, dioxane, reflux. (E) 10% aq.

HCl, 40 °C. (F) AcONH₄, toluene (or AcOH), reflux.

571 3.2 Optical, electrochemical and photophysical properties

572 To gain an insight into the impact the number of polymethine chains and chainlength on the optical and
 573 electrochemical properties of investigated dyes, we have performed UV-vis, FL and cyclic voltammetry

574 studies of di-anchoring dyes **TD1–TD3** and their mono-anchoring analogues **D1–D3** in DMSO. As
575 shown in Figure 3, the absorption spectra of both, di-anchoring organic dyes based on TB scaffold **TD1**,
576 **TD2, TD3** and mono-anchoring dyes **D1–D3** display two distinct absorption bands at around 270–350 nm
577 and 400–670 nm, respectively. The absorption bands in the UV region show shoulders at longer
578 wavelengths correspond to the π – π^* electron transitions of the conjugate system. Interestingly, the
579 sensitizers **TD3** and its mono analogue **D3** exhibit weak but clear additional absorption band at around
580 380 nm. This is a consequence of most extended conjugation made possible by two additional methine
581 units in the present series of dyes. The strong absorption bands in the visible region can be assigned to an
582 intramolecular charge transfer (ICT) between the triphenylamine-based donor and the electron accepting
583 rhodanine-3-acetic acid moiety, providing efficient charge separation at the excited state. Comparison of
584 the absorption spectra of π -extended dyes **TD2, TD3** and **D2, D3** with those of their lower homologues
585 **TD1** and **D1**, clearly demonstrates that the extension of the polymethine chain results in 10–35 nm
586 bathochromic shift of the absorption band compared to that of the lower homologues. Next, comparison
587 of the optical properties of di-anchoring dyes **TD1–TD3** with those of their mono-anchoring analogues
588 **D1–D3** clearly demonstrates two effects. First, the organic dyes based on TB scaffold, with the exception
589 of **TD2**, exhibit approximately twice higher extinction coefficients (Table 1) compared to those of the
590 references mono-anchoring dyes. The molar extinction coefficient of the charge transfer transition in
591 these dyes indicates a good ability for light harvesting. Second, only a negligible bathochromic shift (6 nm)
592 was observed for the di-anchoring dye **TD1** in comparison with mono-anchoring sensitizer **D1**. This
593 indicates that there is no interaction at the ground state between the two chromophores in this di-
594 anchoring dye. However, the comparison of the ICT absorption bands of **TD2** and **TD3** with references
595 **D2** and **D3** clearly indicates this interaction. Probably, this is a consequence of the extended polymethine

596 chains that should ensure flexibility of these units and inspire the interaction between two chromophores
597 in TB-based dyes.

598 Figures S1-S6 show the emission and absorption spectra in the visible region of the dyes in
599 DMSO solution. The excitation wavelength for emission was the maximum absorption in the visible
600 region. It can be seen that the maximum emission wavelengths in DMSO solution follow the order **D1** <
601 **D2** < **D3** and **TD1** < **TD2** < **TD3**. In addition, relatively large Stokes shifts of designing molecules were
602 observed between the absorption and emission spectral maxima. Moreover, the Stokes shifts were
603 calculated to lie within range from 193–276 nm, meaning an enhanced geometrical difference between
604 the ground and excited state geometry and thus a good molecular flexibility of the excited state (Table 1).
605 The Stokes shifts follow the trend **TD3** > **TD2** > **TD1** and **D3** > **D2** > **D1**. In this respect, it is easy to
606 postulate that the largest Stokes shifts found in **TD3** and its mono-analogue **D3** are due to their hexadiene
607 moieties between donor and acceptor that confirms a great flexibility of these dyes.

608

609 *Insert Figure 3*

610

611 The absorption maxima of the investigated dyes on the TiO₂ layer are broader and slightly blue
612 shifted compared to the results obtained in DMSO solutions, indicating that energy levels of the sensitizer
613 molecules have somewhat changed due to the interaction with TiO₂ (Figure 4, Table 1). Upon increasing
614 the number of double bonds from n = 0 to 2, progressive blue shifts are observed for each additional
615 methine unit, leading to the biggest shift of 30 nm for the V-shaped dye **TD3** (from 526 to 496 nm) and
616 14 nm for its reference rod-shaped dye **D3** (from 503 to 489 nm). It shows that H-aggregates form on the
617 TiO₂ surface. The absorption spectrum of mono-anchoring dye **D1** (n = 0) on TiO₂ film shows no
618 difference in comparison with that in DMSO solution implying that there are no evident aggregations. It

619 can be attributed to the size of the molecule. This phenomenon indicates that **D1** may show the highest
620 open-circuit photovoltage value among these six dyes, which is in favor of a better photovoltaic
621 performance.

622 *Insert Figure 4*

623
624 To evaluate the thermodynamic allowed electron transfer processes from the excited dye molecule to
625 the conduction band of TiO₂, cyclic voltammetry (CV) measurements were performed (Table 1, Fig. 5).
626 The cyclic voltammograms of all synthesized compounds show quasi-reversible oxidation and reduction
627 couples. The zero-zero excitation energy ($E_{0,0}$) values were estimated from the cross-point of the
628 normalized UV absorption and photoluminescence spectra [4a]. Adding an additional electron-accepting
629 group in **TD1**, **TD2** and **TD3** decreases the LUMO level by 0.09, 0.34 and 0.18 eV, respectively in
630 comparison with their mono analogues **D1**, **D2** and **D3**. The LUMO energy levels for the dyes lie above
631 the conduction band edge of TiO₂ (-4.0 eV) [19, 28], ensuring favorable electron injection from the
632 excited state of the sensitizers to the conduction band of the semiconductor. The HOMO levels of V-
633 shaped dyes **TD1**, **TD2** and **TD3** (-5.62, -5.58 and -5.51 eV) are more positive than that of their
634 counterparts **D1** (-5.70 eV), **D2** (-5.64 eV) and **D3** (-5.59 eV). Apparently, the HOMO levels of all dyes
635 were more negative than the iodide/triiodide potential (-4.97 eV; -0.54 V vs SHE) [29], which implied
636 that the thermodynamic driving force for the regeneration of the oxidized dyes is sufficient.

637 *Insert Table 1*

638
639 When considering the use of an organic material for optoelectronic applications it is important to
640 have an understanding of its solid-state ionization potential. This understanding can help in identifying
641 suitable organic transport and inorganic electrode materials. The ionization potential (I_p) was measured

642 by the electron photoemission in air method (Fig. 6), and results are presented in Table 1; the
643 measurement error is evaluated as ± 0.03 eV.

644

645 *Insert Figure 5*

646

647 In general, I_p measurements indicate that all investigated sensitizers have very similar energy levels
648 and are in range of 5.38–5.54 eV. From the data presented in Table 1 and Figure 4 it can be stated that I_p
649 values of the dyes based on TB scaffold **TD1** and **TD3** possessing di-anchoring system are the same or
650 really close to their rod-shaped mono-analogues **D1** and **D3**. The ionization potential of **TD2** was
651 determined to be 5.54 eV. It has the highest I_p value of all investigated dyes and the biggest difference of
652 0.16 eV with his mono counterpart **D2** (5.38 eV). Measured I_p values are slightly lower than the HOMO
653 levels found in the CV experiments. The difference may result from different measurement techniques
654 and conditions (solution in CV and solid film in the photoemission method). From the ionization
655 potential and optical band gap ($E_g^{opt-film}$) estimated from the edge of electronic absorption spectra from the thin
656 films the electron affinity (EA) was calculated (Table 1). The expansion of the methine component
657 contributes to higher EA value of the investigated dyes.

658 *Insert Figure 6*

659

660 3.3 Quantum chemistry calculation

661 It is known [20] that Tröger's base has V-shaped twisted configuration with large dihedral angle (80–
662 104°). It displays the huge rigidity and steric hindrance which can restrict internal rotation. Moreover, all
663 the protons on the poly[n]enic backbones are *trans*-geometry, as the TB scaffold-based metal-free

664 sensitizers dye molecules were formed by Horner-Wittig condensation which leads to excellent *E*-
665 geometry selectivity [26]. In addition, according to the literature [33], the synthesis of rhodanine dyes
666 results the thermodynamically more stable *Z*-geometry isomers. Taking into account the above mentioned
667 arguments, we have undertaken a computational study of TB-based two-anchoring dyes. Two possible
668 rotamers were studied for the each of the TB-based dyes. One – “*closed*” form (Figure 7a) is of the
669 minimal energy and employs intramolecular association between two carboxylic acid fragments. In the
670 other “*open*” form (Figure 7b.) substituted diphenylamine fragments were rotated 180° around N-C bond
671 prior to optimization, in order to obtain an association-free rotamer. These geometries were optimized at
672 the B3LYP/def2-SVP level of Density Functional Theory. In the more stable one (“*closed*” form) the
673 rhodanine ring is slightly twisted with respect to the phenyl ring at the triphenylamine and determine the
674 possible internal hydrogen bonding between carboxylic acid moieties prohibiting effective utilization of
675 both anchoring groups. The less stable conformer (“*open*” form) is planar from rhodanine-acceptor to
676 triphenylamine-donor. Optimized geometries of the “*closed*” and “*open*” forms are given in the Table 2.
677 Two rotamers differ by 14.9–16.4 kcal/mol for different dyes, hence association is favorable at room
678 temperature.

679 *Insert Figure 7*

680 HOMO and LUMO orbital plots are shown in Table 2. It can be seen that HOMO orbitals are
681 delocalized over the whole molecule, with the slight shift towards triphenylamine fragments. LUMO
682 orbitals are shifted towards rhodanine fragment. This shows partial charge-transfer character of the
683 HOMO/LUMO transition.

684 *Insert Table 2*

685

686 *3.4. Photovoltaic performance*

687 The photovoltaic performance of the investigated dyes (**TD1–TD3** and **D1–D3**) was then evaluated in
688 DSSCs based on iodide-triiodide electrolyte without any co-adsorbent or co-sensitizer added. Figure 8
689 shows *J-V* characteristics of these DSSCs and the photovoltaic parameters are summarized in Table 3.
690 The cells based on the dye **TD3** and its counterpart **D3** with the longest methine chains showed broader
691 IPCEs (400–700 nm) but lower values (around 7%) compared to other dyes (400–600 nm; 12–40%),
692 resulting in lower J_{sc} values (1.44 and 1.12 mA/cm²).

693

694 *Insert Table 3*

694

695 *Insert Figure 8*

695

696

697 The cells fabricated with the di-anchoring dyes, except of **TD3**, showed slightly lower V_{oc} values to
698 those with the mono-anchoring dyes. It is obvious that J_{sc} - V_{oc} values decreased together with the
699 increasing number of double bonds ($n = 0 > n = 1 > n = 2$) between the donor and acceptor/anchoring
700 group. As it can be assumed from the analyzed optical properties, the best results were obtained using dye
701 **D1**, showing an overall conversion efficiency (η) of 2.36% ($J_{sc} = 5.42 \text{ mA cm}^{-2}$, $V_{oc} = 582 \text{ mV}$, $FF =$
702 0.75). It is obvious, that the reduced tendency of dye aggregate formation is the main factor influencing
703 better DSSC characteristics. Interestingly, additional acceptor-anchor units in sensitizers **TD1**, **TD2** did
704 not have a positive effect on device performance; overall, DSSC efficiencies are noticeably lower
705 compared with mono-anchoring dyes **D1**, **D2**.

706

707 4. Conclusions

708 We have designed and synthesized a series of novel metal-free di-anchoring organic dyes based on a
709 Troger's base scaffold (**TD1**, **TD2**, **TD3**) possessing triphenylamine donor and rhodanine-3-acetic acid as
710 acceptor/anchoring group being linked by the poly[n]enic (from $n = 0$ to 2) chain. The influence of the
711 polymethine chain length and number of the anchoring groups on the photophysical, electrochemical, and
712 photovoltaic properties of these V-shape sensitizers was investigated. Therefore, it has been proven that
713 the extended polymethine chains ensure flexibility of these units and inspire the interaction between two
714 chromophores promoting aggregate formation in these Troger's base-based dyes. Therefore, the best
715 result of DSSCs, showing an overall conversion efficiency of 2.36%, was obtained using dye **D1**
716 possessing the shortest polymethine chain length and one anchoring group.

717 Further studies will be focused on chaining the polymethine backbones by bulky structural moieties,
718 which should protect aggregate formation in di-anchoring organic dyes based on Troger's base scaffold.

719

720 Acknowledgements

721 The authors acknowledge funding from the Research Council of Lithuania (grant No. MIP-105/2015).

722 References

723 [1] (a) Nazeeruddin MK, De Angelis F, Fantacci S, Selloni A, Viscardi G, Grätzel M, et al. Combined
724 experimental and DFT-TDDFT computational study of photoelectrochemical cell ruthenium sensitizers. *J*
725 *Am Chem Soc* 2005;127(48):16835–47; (b) Nazeeruddin MK, Péchy P, Renouard T, Zakeeruddin SM,
726 Grätzel M, et al. Engineering of efficient panchromatic sensitizers for nanocrystalline TiO₂-based solar
727 cells. *J Am Chem Soc* 2001;123(8):1613–24.

- 728 [2] Yella A, Lee HW, Tsao HN, Yi CY, Chandiran A, Nazeeruddin MK, et al. Porphyrin-sensitized solar
729 cells with cobalt (II/III)-based redox electrolyte exceed 12 percent efficiency. *Science* 2011;334:629–33.
- 730 [3] Yella A, Mai CL, Zakeeruddin SM, Chang SN, Hsieh CH, Yeh CY, Grätzel M. Molecular
731 engineering of push-pull porphyrin dyes for highly efficient dye-sensitized solar cells: the role of benzene
732 spacers. *Angew Chem Int Ed* 2014;53(11):2973–7.
- 733 [4] (a) Dai XX, Feng HL, Chen WJ, Yang Y, Nie LB, Wang L, et al. Synthesis and photovoltaic
734 performance of asymmetric di-anchoring organic dyes. *Dyes Pigment* 2015;122:13–21. (b) Zhang F, Luo
735 YH, Song JS, Guo XZ, Liu WL, Ma CP, et al. Triphenylamine-based dyes for the dye-sensitized solar
736 cells. *Dyes Pigment* 2009;81:224–30. (c) Hagfeldt A, Boschloo G, Sun L, Kloo L, Pettersson H. Dye-
737 sensitized solar cells. *Chem Rev* 2010;110:6595–663.
- 738 [5] Kakiage K, Aoyama Y, Yano T, Otsuka T, Kyomen T, Unno M, et al. An achievement of over 12
739 percent efficiency in an organic dye-sensitized solar cell. *Chem Commun* 2014;50:6379–81.
- 740 [6] (a) Baheti A, Justin Thomas KR, Li CT, Lee CP, Ho KC. Fluorene-based sensitizers with a
741 phenothiazine donor: effect of mode of donor tethering on the performance of dye-sensitized solar cells.
742 *ACS Appl Mater Interfaces* 2015;7(4):2249–62; (b) Liang M, Chen J. Arylamine organic dyes for dye-
743 sensitized solar cells. *Chem Soc Rev* 2013;42:3453–88; (c) Mishra A, Fischer MKR, Bauerle P.
744 Metal-free organic dyes for dye-sensitized solar cells: from structure: property relationships to design
745 rules. *Angew Chem Int Ed* 2009;48:2474–99.
- 746 [7] Jia H, Shen K, Ju X, Zhang M, Zheng H. Enhanced performance of dye-sensitized solar cells with Y-
747 shaped organic dyes containing di-anchoring groups. *New J Chem* 2016;40:2799–2805.

- 748 [8] Ooyama Y, Harima Y. Photophysical and electrochemical properties, and molecular structures of
749 organic dyes for dye-sensitized solar cells. *Chem Phys Chem* 2012;13(18):4032–80.
- 750 [9] Tian H, Yang X, Chen R, Zhang R, Hagfeldt A, Sun L. Effect of different dye baths and dye-
751 structures on the performance of dye-sensitized solar cells based on triphenylamine dyes. *J Phys Chem C*
752 2008;112(29):11023–33.
- 753 [10] Ren X, Jiang S, Cha M, Zhou G, Wang ZS. Thiophene-bridged double D- π -A dye for efficient dye-
754 sensitized solar cell. *Chem Mater* 2012;24:3493–9.
- 755 [11] Wu G, Kong F, Zhang Y, Zhang X, Li J, Chen W, et al. Effect of different acceptors in di-anchoring
756 triphenylamine dyes on the performance of dye-sensitized solar cells. *Dyes Pigment* 2014;105:1–6.
- 757 [12] Abbotto A, Manfredi N, Marini C, De Angelis F, Mosconi E, Yum JH, et al. Di-branched di-
758 anchoring organic dyes for dye-sensitized solar cells. *Energy Environ Sci* 2009;2:1094–1101.
- 759 [13] Sirohi R, Kim DH, Yu SC, Lee SH. Novel di-anchoring dye for DSSC by bridging of two mono
760 anchoring dye molecules: A conformational approach to reduce aggregation. *Dyes Pigment*
761 2012;92:1132–37.
- 762 [14] Dai XX, Feng HL, Huang ZS, Wang MJ, Wang L, Kuang DB, et al. Synthesis of phenothiazine-
763 based di-anchoring dyes containing fluorene linker and their photovoltaic performance. *Dyes Pigments*
764 2015;114:47–54.
- 765 [15] Urnikaite S, Malinauskas T, Bruder I, Send R, Gaidelis V, Sens R, Getautis V. Organic dyes with
766 hydrazone moieties: a study of correlation between structure and performance in the solid-state dye-
767 sensitized solar cells. *J Phys Chem C* 2014;118:7832–43.

- 768 [16] Pardo C, Sesmilo E, Gutiérrez-Puebla E, Monge A, Elguero J, Fruchier A. New chiral molecular
769 tweezers with a bis-Tröger's base skeleton. *J Org Chem* 2001;66(5):1607–11.
- 770 [17] Goswami S, Gosh K, Disrupt S. Troger's base molecular scaffolds in dicarboxylic acid recognition. *J*
771 *Org Chem* 2000;65(7):1907–14.
- 772 [18] Rúnarsson ÖV, Artacho J, Wärnmark K. The 125th anniversary of the tröger's base molecule:
773 synthesis and applications of tröger's base analogues. *Eur J Org Chem* 2012;7015–41.
- 774 [19] Braukyla T, Sakai N, Daskeviciene M, Jankauskas V, Kamarauskas E, Malinauskas T, Snaith HJ,
775 Getautis V. Synthesis and investigation of the V-shaped Tröger's base derivatives as hole-transporting
776 materials. *Chem An Asian J* 2016;11(14):2049-2056.
- 777 [20] (a) Faroughi M, Try AC, Turner P. 2,8-Dibromo-6*H*,12*H*-5,11-methanodibenzo-*[b,f]*[1,5]diazocine.
778 *Acta Cryst* 2006;E62:o3674–o3675. (b) Ramirez CL, Pegoraro C, Trupp L, Bruttomesso A, Amorebieta
779 V, Vera DM, Parise AR. Charge transfer properties of Tröger base derivatives. *Phys Chem Chem Phys*
780 2011;13:20076–80.
- 781 [21] Lee MW, Cha SB, Yang SJ, Park SW, Kim K, Park NG, Lee DH. Synthesis of Organic Dyes with
782 Linkers Between 9,9-Dimethylfluorenyl Terminal and α -Cyanoacrylic Acid Anchor, Effect of the Linkers
783 on UV-Vis Absorption Spectra, and Photovoltaic Properties in Dye-Sensitized Solar Cells. *Bull Korean*
784 *Chem Soc* 2009;30(10): 2269–79.
- 785 [22] Jensen J, Wärnmark K. Synthesis of Halogen Substituted Analogues of Tröger's Base. *Synthesis*
786 2001;12:1873–77.

- 787 [23] Miyamoto E, Yamaguchi Y, Yokoyama M. Ionization potential of organic pigment film by
788 atmospheric photoelectron emission analysis. *Electrophotogr* 1989;28:364–70.
- 789 [24] Daskeviciene M, Getautis V, Grazulevicius VJ, Stanisauskaite A, Antulis J, Gaidelis V, et al.
790 Crosslinkable carbazolyl-containing molecular glasses for electrophotography. *J Imaging Sci Technol*
791 2002;46:467–72.
- 792 [25] (a) Ahlrichs R, Bär M, Häser M, Horn H, Kölmel C. Electronic structure calculations on workstation
793 computers: The program system turbomole. *Chem Phys Lett* 1989;162:165–9. (b) Lee C, Yang W, Parr
794 RG. Development of the Colle-Salvetti correlation-energy formula into a functional of the electron
795 density. *Phys Rev B* 1988;37:785–9. (c) Becke AD. Density-functional thermochemistry. III. The role of
796 exact exchange. *J Chem Phys* 1993;98:5648–52. (d) Schäfer A, Horn H, Ahlrichs R. Fully optimized
797 contracted Gaussian basis sets for atoms Li to Kr. *J Chem Phys* 1992;97:2571–7. (e) Weigend F, Ahlrichs
798 R, Weigend F, Furche F, Ahlrichs R, Leininger T, et al. Balanced basis sets of split valence, triple zeta
799 valence and quadruple zeta valence quality for H to Rn: Design and assessment of accuracy. *Phys Chem*
800 *Chem Phys* 2005;7:3297. (f) Steffen C, Thomas K, Huniar U, Hellweg A, Rubner O, Schroer A. TmoleX-
801 A graphical user interface for TURBOMOLE. *J Comput Chem* 2010;31:2967–70.
- 802 [26] Parthasarathy V, Pandey R, Stotle M, Ghosh S, Castet F, Würthner F, Das PK, Desce MB.
803 Combination of Cyanine Behaviour and Giant Hyperpolarisability in Novel Merocyanine Dyes: Beyond
804 the Bond Length Alternation (BLA) Paradigm. *Chem A Eur J* 2015;21(40):14211–17.
- 805 [27] Pernille H. Poulsen, Karla Santos Feu, Bruno Matos Paz, Frank Jensen, and Karl Anker Jørgensen,
806 Organocatalytic Asymmetric 1,6-Addition/1,4-Addition Sequence to 2,4-Dienals for the Synthesis of
807 Chiral Chromans. *Angew. Chem. Int. Ed.* 2015, 54, 8203–8207.

- 808 [28] Qin P, Tetreault N, Dar MI, Gao P, McCall KL, Rutter SR, et al. A Novel Oligomer as a Hole
809 Transporting Material for Efficient Perovskite Solar Cells. *Adv Energy Mater* 2015;5(2):1400980.
- 810 [29] LeBlanc SE, Fogler HS. The Role of Conduction/Valence Bands and Redox Potential in Accelerated
811 Mineral Dissolution. *AIChE J* 1986;32(10):1702–09.
- 812 [30] Connelly N, Geiger W. Chemical Redox Agents for Organometallic Chemistry. *Chem Rev*
813 1996;96:877–910.
- 814 [31] Pavlishchuk V, Addison A. Conversion constants for redox potentials measured versus different
815 reference electrodes in acetonitrile solutions at 25°C. *Inorganica Chimica Acta* 2000;298:97–102.
- 816 [32] Reiss H, Heller A. The absolute potential of the standard hydrogen electrode: a new estimate. *J Phys*
817 *Chem* 1985;89:4207–13.
- 818 [33] (a) Dolezel J, Hirsova P, Opletalova B, Dohnal J, Marcela V, Kunes J, Jampilek J. Rhodanineacetic
819 Acid Derivatives as Potential Drugs: Preparation, Hydrophobic Properties and Antifungal Activity of (5-
820 Arylalkylidene-4-oxo-2-thioxo-1,3-thiazolidin-3-yl)acetic Acids. *Molecules* 2009;14:4197–4212; (b)
821 Peng B, Yang S, Li L, Cheng F, Chen J. A Density Functional Theory and Time-Dependent Density
822 Functional Theory Investigation on the Anchor Comparison of Triarylamine-Based Dyes. *J Chem Phys*
823 2010;132:034305–14.
- 824
- 825
- 826
- 827
- 828

- 829 **Table and figure captions**
- 830 **Table 1.** Optical and electrochemical properties data of investigated dyes.
- 831 **Table 2.** Optimized structures and frontier molecular orbitals of di-anchoring dyes **TD1–TD3**.
- 832 **Table 3.** Photovoltaic performance of DSSCs based on the different dyes under $100 \text{ mW}\cdot\text{cm}^{-2}$ AM1.5 G
833 illumination.
- 834 **Figure 1.** Molecular structures of reported sensitizers.
- 835 **Figure 2.** Molecular structures of investigated dyes **TD1, TD2, TD3, D1, D2** and **D3**.
- 836 **Figure 3.** UV/vis spectra of investigated dyes **TD1–TD3** and **D1–D3** in DMSO solutions ($c = 10^{-4} \text{ M}$).
- 837 **Figure 4.** Normalized absorption of dyes **TD1–TD3** and **D1–D3** anchored on TiO_2 film.
- 838 **Figure 5.** Schematic energy level diagram for a DSSC based on dyes attached to a nanocrystalline TiO_2
839 film deposited on conducting FTO glass.
- 840 **Figure 6.** Photoemission in air spectra of the investigated dyes.
- 841 **Figure 7.** Possible geometry-rotamers of TB-based dye **TD1**: (a) “closed”, (b) “open” .
- 842 **Figure 8.** (a) J - V characteristics of the DSSCs based on dyes **TD1–TD3** and **D1–D3**. (b) IPCE spectra of
843 **TD1–TD3** and **D1–D3** dye-sensitized devices.
- 844
- 845
- 846
- 847
- 848
- 849

850 **Table 1.** Optical and electrochemical properties data of investigated dyes

Dye	$\lambda_{\text{abs}}^{\text{sol}}$ (nm) ^b	ϵ (M ⁻¹ cm ⁻¹)	λ_{max} on TiO ₂ (nm)	λ_{em} (nm) ^b	Stokes shift ^c (nm)	λ_{int} (nm) ^d	E_{0-0} (eV) ^e	$E_g^{\text{opt-film}}$ (eV) ^f	E_{HOMO} (eV) ^a	E_{LUMO} (eV) ^a	I_p (eV) ^g	EA (eV) ^h
TD1	307, 475	36 382, 71 369	468	689	221	541	2.29	2.07	-5.62	-3.36	5.48	-3.41
TD2	298, 510	56 510, 44 680	506	714	208	585	2.12	1.80	-5.58	-3.76	5.54	-3.74
TD3	302, 389, 526	43 360, 23 040, 68 550	496	763	267	631	1.96	1.68	-5.51	-3.65	5.45	-3.77
D1	307, 469	14 679, 37 956	469	662	193	530	2.34	2.07	-5.70	-3.27	5.43	-3.36
D2	304, 493	13 270, 37 190	483	712	229	571	2.17	1.84	-5.64	-3.42	5.38	-3.54
D3	308, 503	14 740, 26 190	489	765	276	603	2.05	1.73	-5.59	-3.47	5.45	-3.72

851 The CV measurements were carried out at a glassy carbon electrode in tetrahydrofuran solutions containing 0.1 M
852 tetrabutylammonium hexafluorophosphate as electrolyte and Pt as the reference and counter electrodes. Each
853 measurement was calibrated with ferrocene (Fc). Potentials measured vs Fc+/Fc. ^aConversion factors: ferrocene in
854 THF vs SCE 0.56^[30], SCE vs SHE: 0.244^[31], SHE vs. vacuum: 4.43^[32]. ^bAbsorption and emission spectra were
855 measured in DMSO solution. ^cStokes shift = $\lambda_{\text{em}}(\text{solution}) - \lambda_{\text{abs}}(\text{solution})$. ^d λ intersection obtained from the cross point of
856 normalized absorption and emission spectra in DMSO solution. ^e $E_{0-0} = 1240/\lambda$ intersection. ^fOptical band gap ($E_g^{\text{opt-}}$
857 ^{film}) estimated from the edge of electronic absorption spectra from thin film. ^gIonization potential (I_p) was measured
858 by the photoemission in air method from films. ^hElectron affinity (EA) calculated from the equation $EA = I_p - E_g^{\text{opt-}}$
859 ^{film}.

860

861

862

863

864

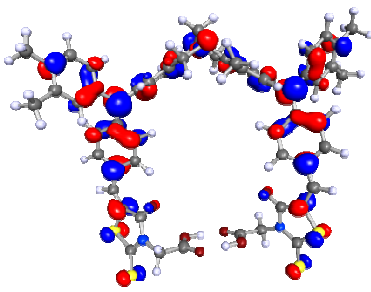
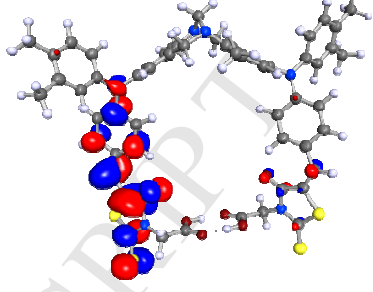
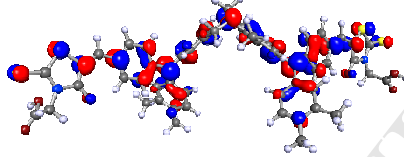
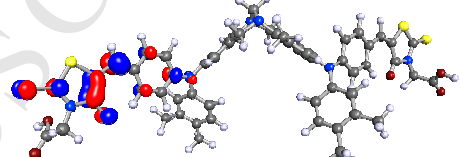
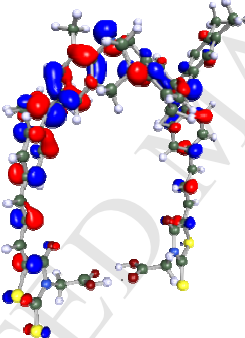
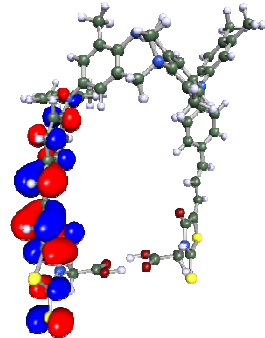
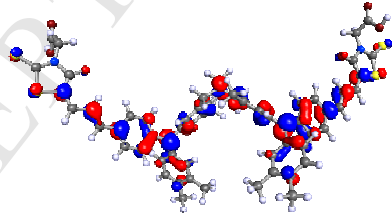
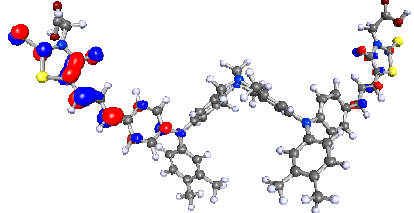
865

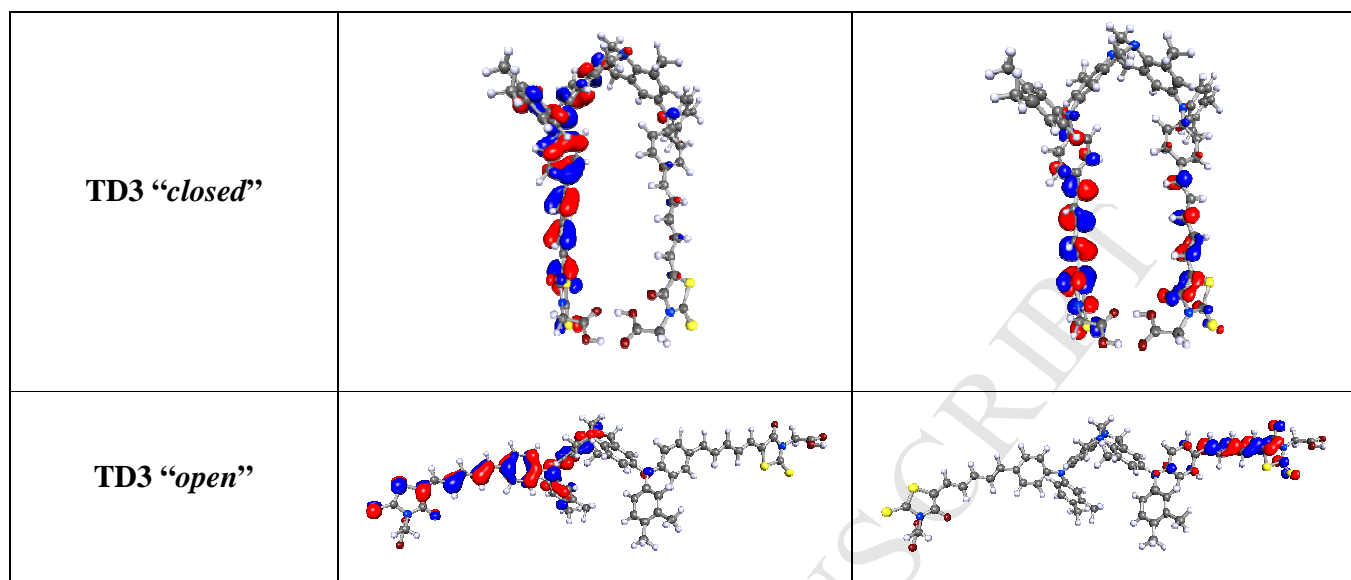
866

867

868

869 **Table 2.** Optimized structures and frontier molecular orbitals of di-anchoring dyes **TD1–TD3**.

DYE	HOMO	LUMO
TD1 “closed”		
TD1 “open”		
TD2 “closed”		
TD2 “open”		



870

871

872

873

874

875

876

877

878

879

880

881

882

883

884

885

886

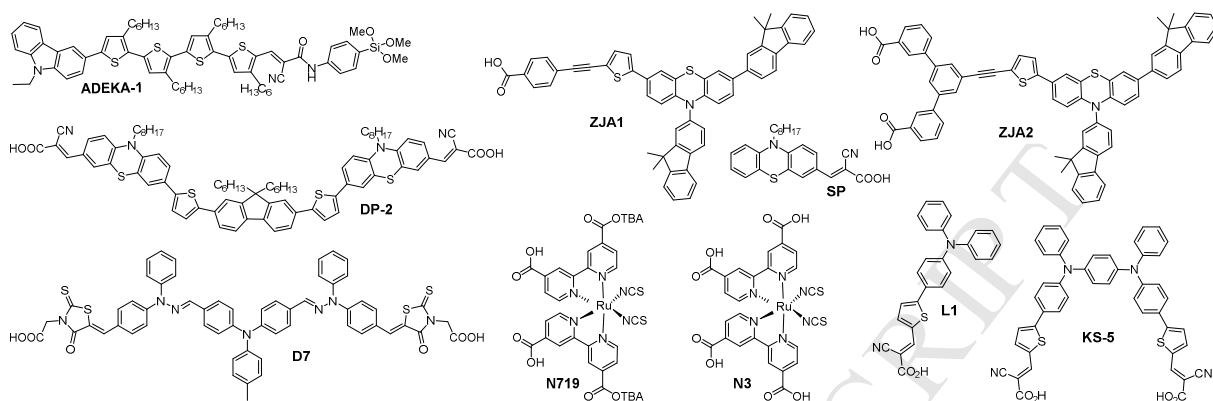
887

888 **Table 3.** Photovoltaic performance of DSSCs based on the different dyes
889 under $100 \text{ mW} \cdot \text{cm}^{-2}$ AM1.5 G illumination.

Dyes	V_{oc} (mV)	J_{sc} (mA/cm ²)	FF (%)	η (%)
TD1	548±3	4.30±0.06	75.9±1.7	1.79±0.05
TD2	468±6	1.99±0.11	73.1±0.9	0.68±0.04
TD3	460±0	1.44±0.04	74.9±0.2	0.50±0.02
D1	582±3	5.42±0.15	75.3±1.5	2.36±0.05
D2	482±3	2.52±0.13	75.2±0.7	0.91±0.06
D3	448±3	1.12±0.10	72.1±0.3	0.36±0.03

890
891
892
893
894
895
896
897
898
899
900
901
902
903
904
905
906
907
908
909
910
911

912



913

914

915

916

917

918

919

920

921

922

923

924

925

926

927

928

929

930

931

932

933

Figure 1. Molecular structures of reported sensitizers.

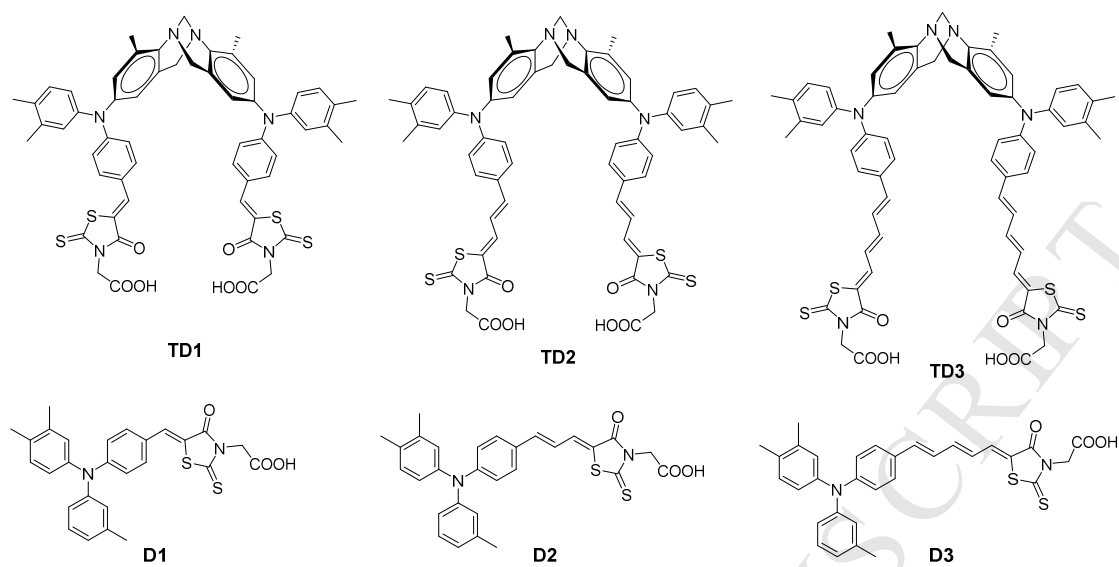
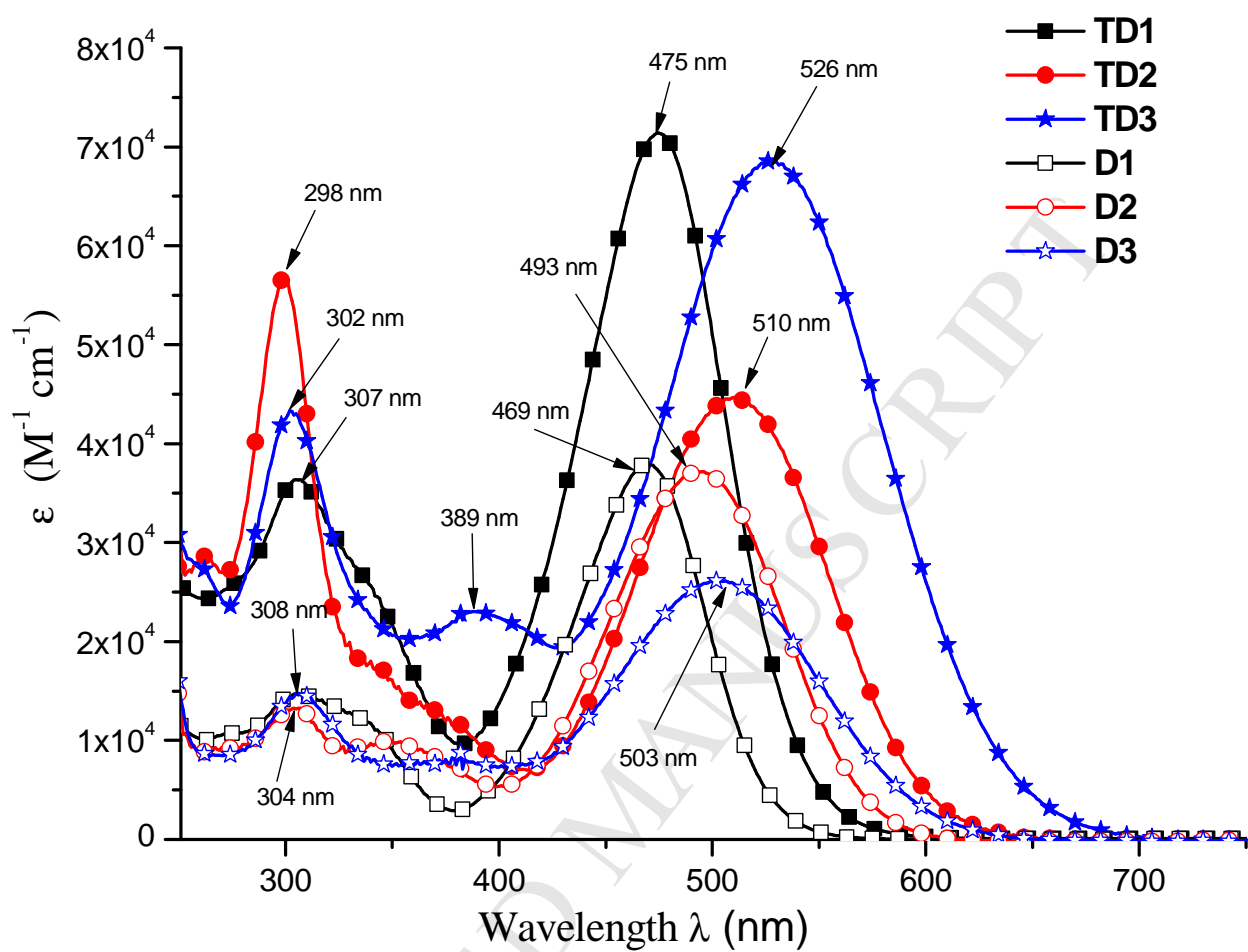


Figure 2. Molecular structures of investigated dyes **TD1**, **TD2**, **TD3**, **D1**, **D2** and **D3**.



950

951

952

953

954

955

956

957

958

959

960

961

962

963

964

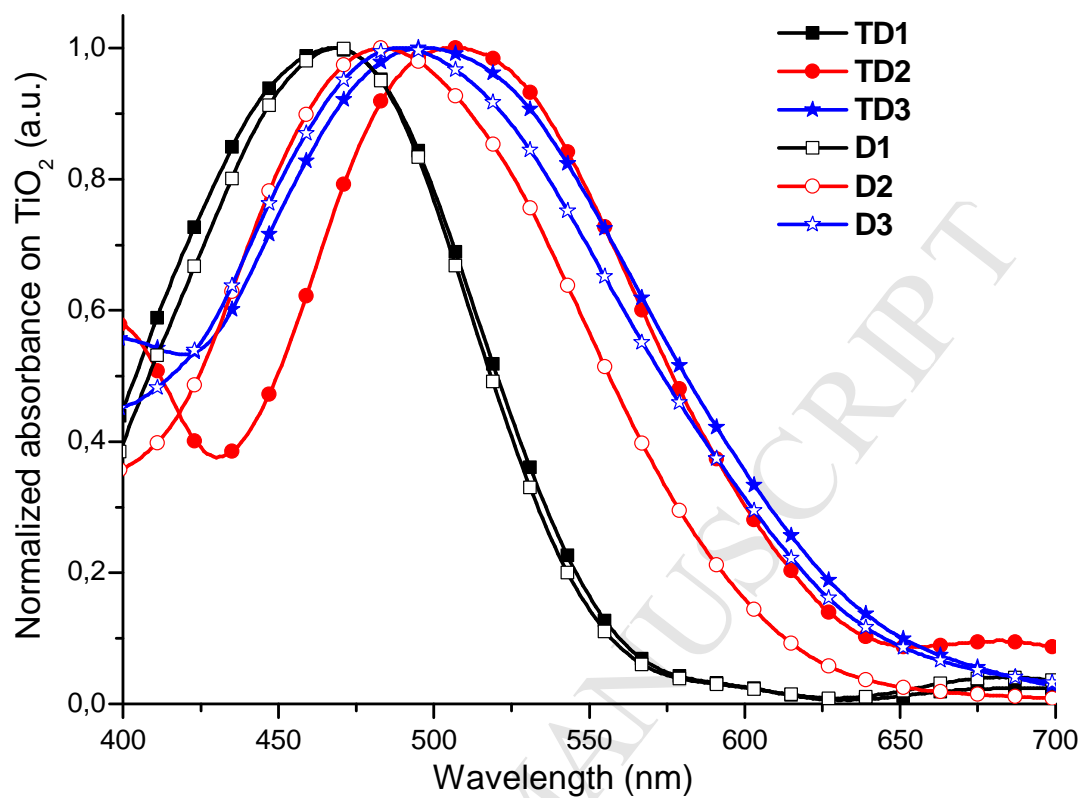
965

966

967

968

Figure 3. UV/vis spectra of investigated dyes TD1–TD3 and D1–D3 in DMSO solutions (c = 10⁻⁴ M).



969

970

971

972

973

974

975

976

977

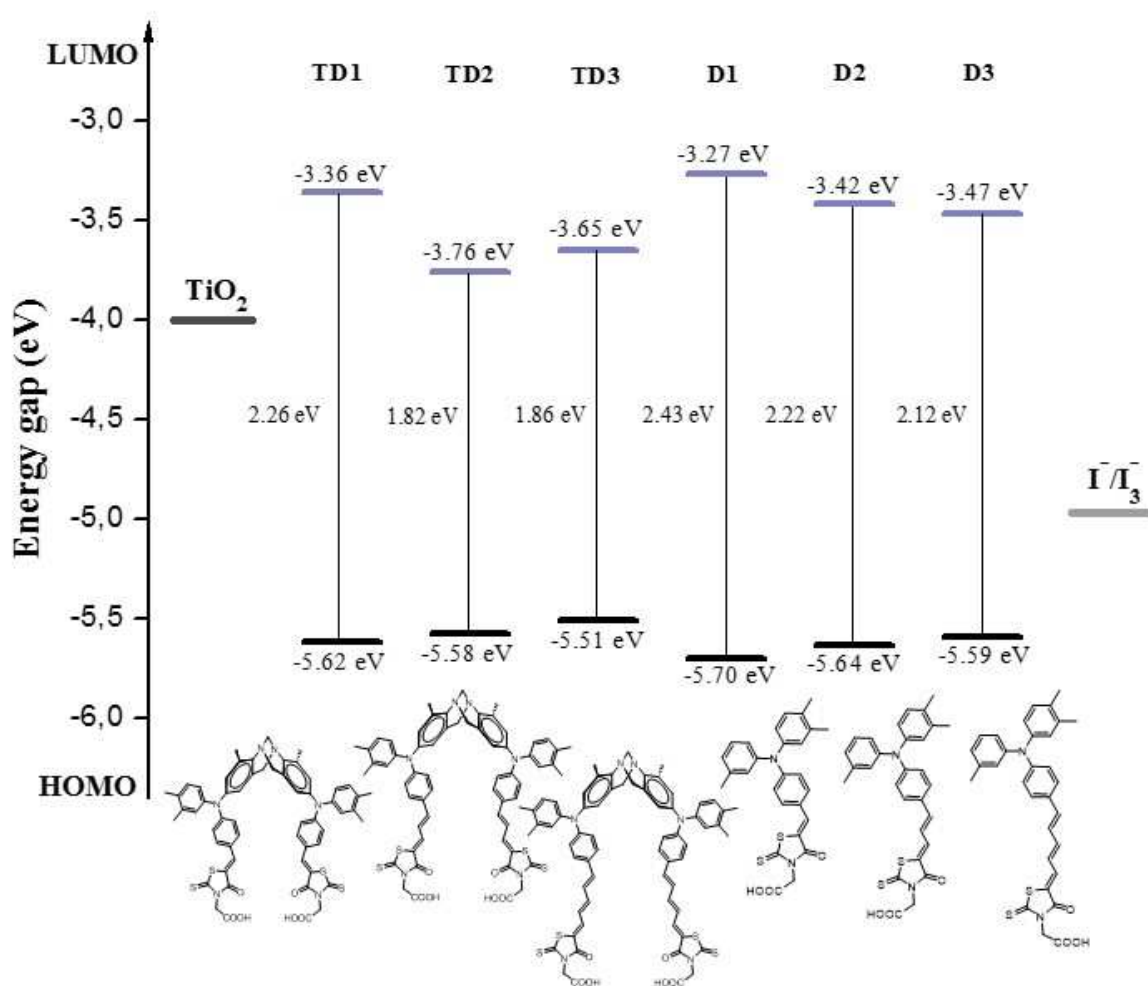
978

979

980

981

Figure 4. Normalized absorption of dyes TD1-TD3 and D1-D3 anchored on TiO₂ film.



982

983

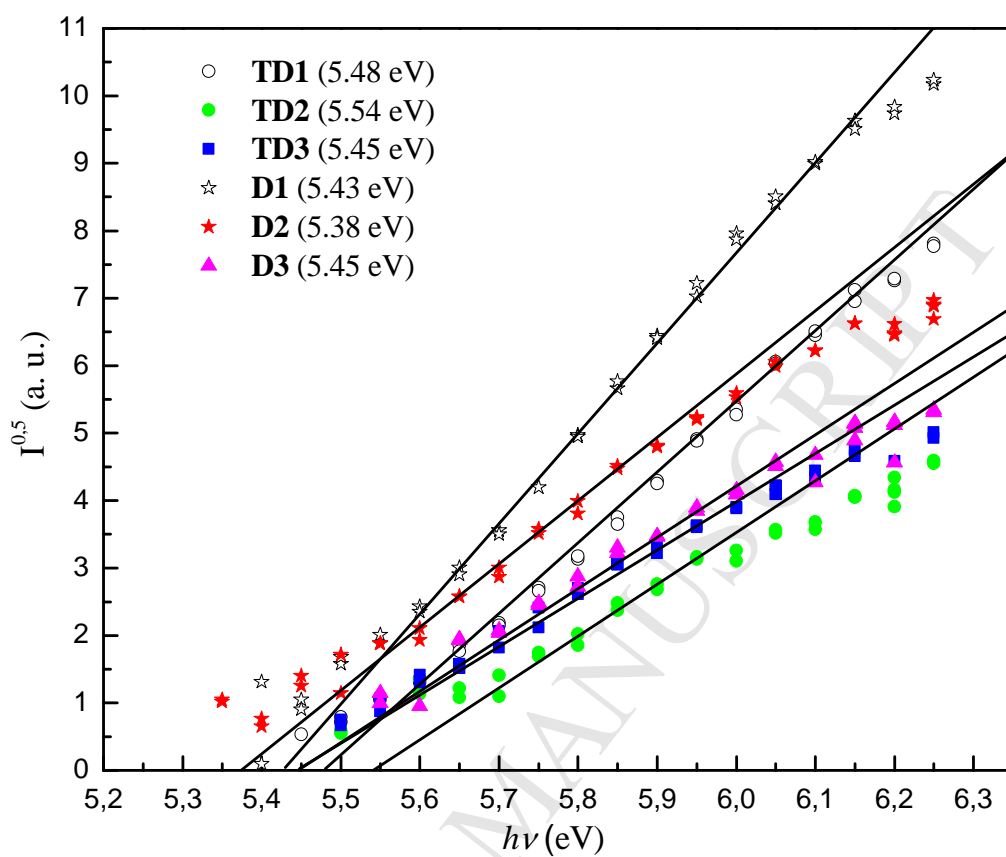
984

985

986

987 **Figure 5.** Schematic energy level diagram for a DSSC based on dyes attached to a nanocrystalline TiO₂

988 film deposited on conducting FTO glass.



989

990

991

992

993

994

995

996

997

998

999

1000

Figure 6. Photoemission in air spectra of the investigated dyes.

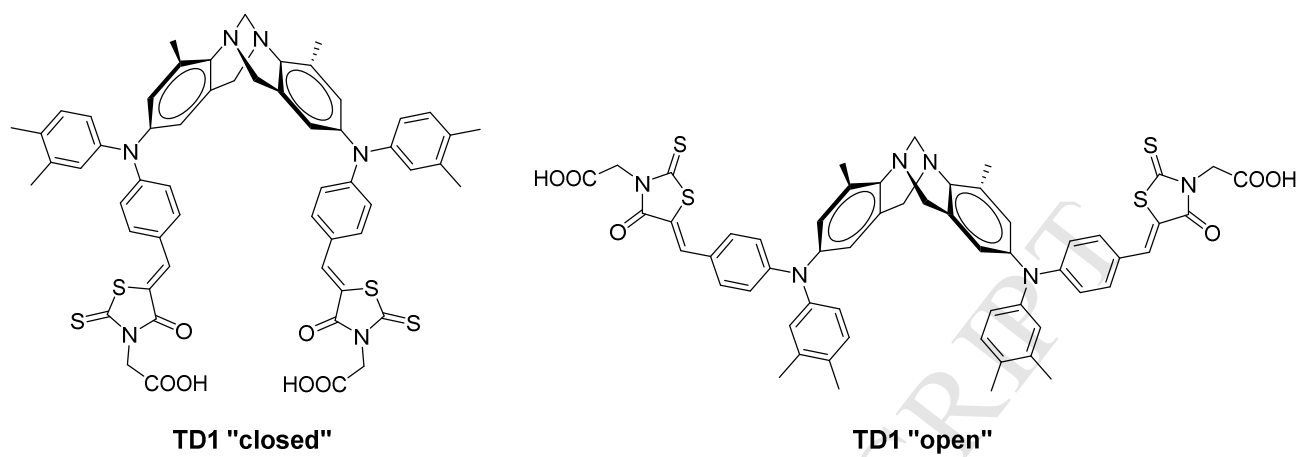
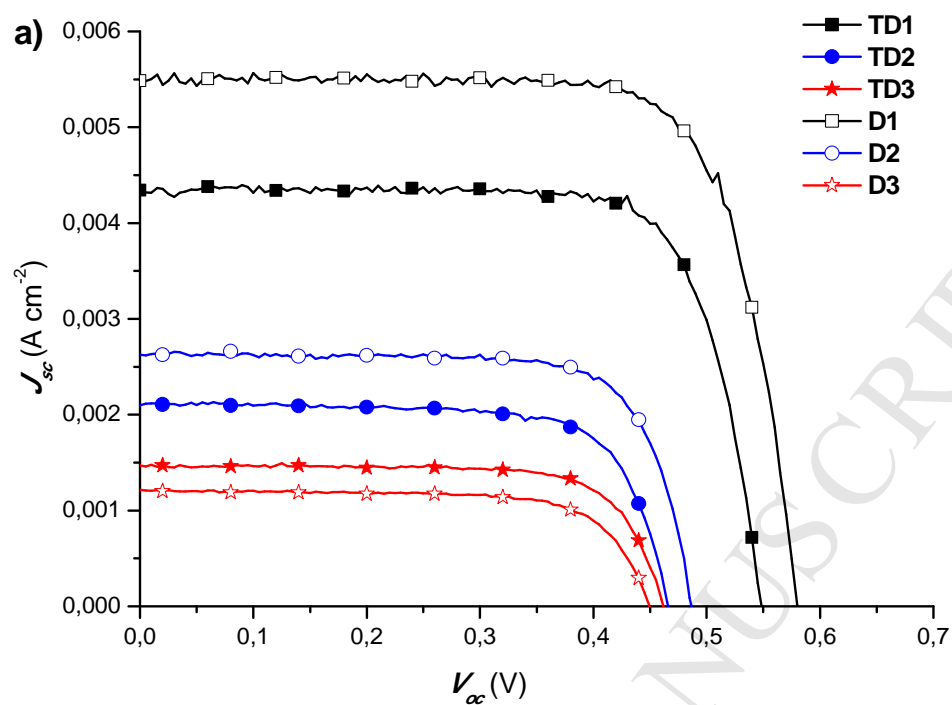
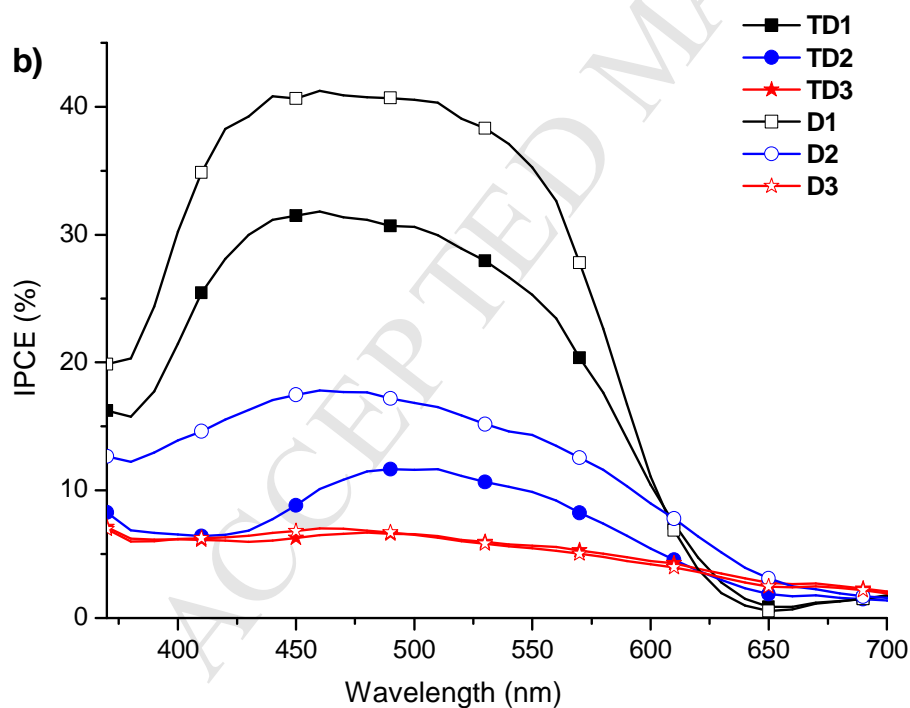


Figure 7. Possible geometry-rotamers of TB-based dye **TD1**: (a) "closed", (b) "open"



1013



1014

1015 **Figure 8.** (a) J - V characteristics of the DSSCs based on dyes **TD1–TD3** and **D1–D3**. (b) IPCE
 1016 spectra of **TD1–TD3** and **D1–D3** dye-sensitized devices.

Highlights

- Novel D- π -A two-anchoring dyes based on Troger's base scaffold were synthesized.
- Two anchor groups are not always better than one.
- A poly[n]enic (from $n = 0$ to 2) chain unit as π -linker inspires the interaction between two chromophores promoting aggregate formation.
- Photovoltaic performance can be influenced by π -linker length and number significantly.